Mutations in M2 Alter the Selectivity of the Mouse Nicotinic Acetylcholine Receptor for Organic and Alkali Metal Cations

BRUCE N. COHEN, CESAR LABARCA, NORMAN DAVIDSON, and HENRY A. LESTER

From the Division of Biology 156-29, California Institute of Technology, Pasadena, California 91125

ABSTRACT We measured the permeability ratios (P_X/P_{Na}) of 3 wild-type, 1 hybrid, 2 subunit-deficient, and 22 mutant nicotinic receptors expressed in *Xenopus* oocytes for alkali metal and organic cations using shifts in the biionic reversal potential of the macroscopic current. Mutations at three positions (2′, 6′, 10′) in M2 affected ion selectivity. Mutations at position 2′ (αThr244, βGly255, γThr253, δSer258) near the intracellular end of M2 changed the organic cation permeability ratios as much as twofold and reduced P_{Cs}/P_{Na} and P_K/P_{Na} by 16–18%. Mutations at positions 6′ and 10′ increased the glycine ethyl ester/Na^+ and glycine methyl ester/Na^+ permeability ratios. Two subunit alterations also affected selectivity: omission of the δ subunit reduced P_{Cs}/P_{Na} by 16%, and substitution of *Xenopus* δ for mouse δ increased $P_{guanidinium}/P_{Na}$ more than twofold and reduced P_{Cs}/P_{Na} by 34% and P_{Li}/P_{Na} by 20%. The wild-type mouse receptor displayed a surprising interaction with the primary ammonium cations; relative permeability peaked at a chain length equal to four carbons. Analysis of the organic permeability ratios for the wild-type mouse receptor shows that (*a*) the diameter of the narrowest part of the pore is 8.4 Å; (*b*) the mouse receptor departs significantly from size selectivity for monovalent organic cations; and (*c*) lowering the temperature reduces $P_{guanidinium}/P_{Na}$ by 38% and $P_{butylammonium}/P_{Na}$ more than twofold. The results reinforce present views that positions −1′ and 2′ are the narrowest part of the pore and suggest that positions 6′ and 10′ align some permeant organic cations in the pore in an interaction similar to that with channel blocker, QX-222.

INTRODUCTION

Three lines of evidence suggest that the M2 transmembrane region lines the pore of the nicotinic acetylcholine receptor (nAChR). (*a*) The noncompetitive antagonists [^{3}H]chlorpromazine and [^{3}H]triphenylmethylphosphonium photolabel residues in M2 (Giraudat, Dennis, Heidmann, Chang, and Changeux, 1986; Hucho, Oberthür,

Address reprint requests to Dr. Henry A. Lester, Division of Biology 156-29, California Institute of Technology, Pasadena, CA 91125.

J. GEN. PHYSIOL. © The Rockefeller University Press · 0022-1295/92/09/0373/28 $2.00
Volume 100 September 1992 373–400

and Lottspeich, 1986; Oberthür, Muhn, Baumann, Lottspeich, Wittman-Liebold, and Hucho, 1986; Giraudat, Dennis, Heidmann, Haumont, Lederer, and Changeux, 1987; Giraudat, Galzi, Revah, Changeux, Haumont, and Lederer, 1989; Revah, Galzi, Giraudat, Haumont, Lederer, and Changeux, 1990); (*b*) mutations in M2 affect single-channel conductance and ion selectivity (Imoto, Methfessel, Sakmann, Mishina, Mori, Konno, Fukuda, Kurasaki, Bujo, Fujita, and Numa, 1986; Imoto, Busch, Sakmann, Mishina, Konno, Nakai, Bujo, Mori, Fukuda, and Numa, 1988; Leonard, Labarca, Charnet, Davidson, and Lester, 1988; Charnet, Labarca, Leonard, Vogelaar, Czyzyk, Gouin, Davidson, and Lester, 1990; Imoto, Konno, Nakai, Wang, Mishina, and Numa, 1991; Konno, Busch, von Kitzing, Imoto, Wang, Nakai, Mishina, Numa, and Sakmann, 1991; Villarroel, Herlitze, Koenen, and Sakmann, 1991; Cohen, Labarca, Czyzyk, Davidson, and Lester, 1992); and (*c*) mutations in M2 affect block of the nAChR by QX-222 (Leonard et al., 1988; Charnet et al., 1990). M1 may also form part of the pore lining (DiPaola, Kao, and Karlin, 1990).

Furthermore, the ion selectivity filter of the nAChR seems to be located near the intracellular end of the M2 transmembrane segment. Mutations at two positions ($-1'$ and $2'$; see Fig. 1) near the intracellular end of M2 affect the single-channel conductance ratios of nAChRs for alkali metal cations (Konno et al., 1991; Villarroel et al., 1991); and a mutation that removes a negative charge at position $-1'$ in the *Torpedo* nAChR $(\alpha\beta\gamma\delta_{E-1'Q})_T$ reduces the permeability of Rb^+ and Cs^+ relative to K^+ (Konno et al., 1991). The equivalent mutation at position $-1'$ in the mouse nAChR ($\alpha\beta\gamma\delta_{E-1'Q}$) and several other mutations at position $2'$ reduce the relative permeability to $Tris^+$ (P_{Tris}/P_{Na}) as much as twofold. Mutations at positions $6'$, $10'$, $12'$, and $14'$ in M2 do not affect P_{Tris}/P_{Na} (Cohen et al., 1992).

The nAChR is permeable to a wide variety of monovalent organic cations (Huang, Catterall, and Ehrenstein, 1978; Dwyer, Adams, and Hille, 1980); we expected that some of these ions would constitute useful probes for additional features of permeation. Moreover, there are no data on the effects of position $2'$ mutations on alkali metal permeability ratios. Therefore, we examined the effects of mutations and subunit alterations on the relative permeability of the mouse nAChR ($\alpha\beta\gamma\delta$) to a variety of organic cations (besides $Tris^+$) and to the alkali metals. Given the widespread use of the *Xenopus* expression system, we also felt that it was worthwhile to repeat the detailed characterization of monovalent organic selectivity performed previously on frog endplate receptors (Dwyer et al., 1980) on $\alpha\beta\gamma\delta$ to determine if there are (*a*) differences among the ion selectivities of the wild-type nAChRs and (*b*) differences between nAChRs expressed heterologously and in their native tissue. For the sake of simplicity, the wild-type mouse subunits are not subscripted in the text.

The results show that positions $-1'$, $2'$, $6'$, and $10'$ in M2 affect ion selectivity. We continue to suggest that positions $-1'$ and $2'$ form the narrowest part of the pore; we now suggest that positions $6'$ and $10'$ facilitate the passage of some organic cations through this narrow region by increasing the probability that the cations are in a favorable orientation for permeation. The results also show that (*a*) $\alpha\beta\gamma\delta$ is not strictly size selective for organic cations; (*b*) temperature affects the relative permeability of the mouse nAChR to some organic cations (guanidinium and butylammonium); and (*c*) other organic cations (amylammonium and *n*-propylammonium) block $\alpha\beta\gamma\delta$. Excluded-area analysis of 12 organic permeability ratios further suggests that

the diameter of the narrowest region of $\alpha\beta\gamma\delta$ is similar to the diameter of the narrowest region of the frog endplate receptor and the narrowest region of the wild-type *Torpedo* receptor $(\alpha\beta\gamma\delta)_T$.

METHODS

The methods used were similar to those of Cohen et al. (1992). We injected oocytes with in vitro transcribed mRNA (2–19 ng per subunit) and incubated the oocytes for 2–10 d in a modified Barth's solution (96 mM NaCl, 2 mM KCl, 1.8 mM $CaCl_2$, 1 mM $MgCl_2$, 2.5 mM Na pyruvate, and 5 mM HEPES at pH 7.4). Point mutations of $\alpha\beta\gamma\delta$ were made using standard techniques (Charnet et al., 1990). The mutations are denoted in the text by subscripts of the mutated subunit. For example, $\delta_{S2'F}$ represents a mutated δ subunit where phenylalanine (F) replaced the original serine (S) at position 2′.

We studied the oocytes with a voltage-clamp circuit that used two KCl-filled microelectrodes and measured membrane voltage differentially with an extracellular 1 M KCl salt bridge as a voltage reference electrode. All data were obtained at ambient temperature (23–25°C) unless otherwise indicated. We generated macroscopic *I-V* relations by ramping the membrane potential over a total range of 60–120 mV during a 0.9-s interval. The current signal was passed through an 8-pole Bessel filter (corner frequency 100–250 Hz) and then digitized at 1 kHz. An MS-DOS computer, equipped with pCLAMP software (V5.5; Axon Systems, Inc., Foster City, CA), recorded the voltage-clamp currents. We averaged the currents from three sequential ramps digitally. The mean current with acetylcholine (ACh) was subtracted from the current without ACh to obtain the difference current, I_{ACh}. This procedure eliminated the background resistive and capacitive (CdV/dt) current. The biionic reversal potential (V_r) of this current was measured directly from the digitized difference current or by fitting a straight line to the region around V_r.

We calculated the permeability ratios (P_X/P_{Na}) for the cations from the shift in V_r (ΔV_r) produced by substituting most or all of the external Na^+ with a test cation (X^+) using the following version of the Goldman-Hodgkin-Katz voltage equation:

$$\frac{P_x}{P_{Na}} = \frac{[Na^+]_r 10^{F\Delta V_r/RT} - [Na^+]_t}{[X^+]}$$

where $[Na^+]_r$ and $[Na^+]_t$ are the concentrations of Na^+ in the reference and test solutions; $[X^+]$ is the concentration of cation X^+ in the test solution; and R, T, and F have the usual meanings (Dwyer et al., 1980). The reference solution contained 98 mM NaCl, 1 mM $MgCl_2$, 2 mM NaOH, and 5 mM HEPES (pH 7.4). The test solution contained concentrations of the test cation and Cl^- that were approximately equimolar to the NaCl in the reference solution, 1 mM $MgCl_2$, and 5 mM buffer (HEPES, ACES, MES, or acetate depending on the pH required). If the test cation was available as a free base, then the test solution contained 0 mM Na^+. Otherwise, a small amount of NaOH was added to adjust the test solution to the desired pH. The pH of the organic test solutions was 7.4 unless otherwise indicated. In some cases, pH was lowered to ensure that most organic molecules in solution were protonated. We omitted the concentration of Mg^{2+} in the test and reference solutions from the calculation of P_X/P_{Na}. Previous data show that pH changes (6.3–7.4) and the addition of 1 mM Mg^{2+} do not affect P_{Tris}/P_{Na}.

Tetramethylammonium (TMA^+) is a weak cholinergic agonist (Adams, 1975*a*, *b*) and it produced a large increase in the background current of $\alpha\beta\gamma\delta$-injected oocytes (but not uninjected oocytes) in the absence of ACh. Therefore, we took the current blocked by adding 10 μM *d*-tubocurarine (*d*-TC) to the TMA^+ solution as I_{ACh} and computed P_{TMA}/P_{Na} from V_r for the *d*-TC-sensitive current.

In most experiments, several blockers were added to the test and reference solutions at low concentrations (10^{-4}–10^{-3} M) to suppress the background conductance of the oocytes. Niflumic or flufenamic acid was present at 75 μM (from a 150-mM stock concentration in ethanol) to suppress the background Cl^- conductance of the oocytes (White and Aylwin, 1990), and atropine sulfate (1–10 μM) was added to block activation of the Cl^- current by residual muscarinic receptors (Dascal, 1987). Residual muscarinic responses were, however, very rare.

			MOUSE																				
	-1	0	1	2	3	4	5	6	7	8	9	10	11	12	13	14	15	16	17	18	19	20	21
α	E	K	M	T	L	S	I	S	V	L	L	S	L	T	V	F	L	L	V	I	V	E	L
β	E	K	M	G	L	S	I	F	A	L	L	T	L	T	V	F	L	L	L	L	A	D	K
γ	Q	K	C	T	V	A	T	N	V	L	L	A	Q	T	V	F	L	F	L	V	A	K	K
δ	E	K	T	S	V	A	I	S	V	L	L	A	Q	S	V	F	L	L	L	I	S	K	R
ε	Q	K	C	T	V	S	I	N	V	L	L	A	Q	T	V	F	L	F	L	I	A	Q	K
			TORPEDO																				
α	E	K	M	T	L	S	I	S	V	L	L	S	L	T	V	F	L	L	V	I	V	E	L
β	E	K	M	S	L	S	I	S	A	L	L	A	V	T	V	F	L	L	L	L	A	D	K
γ	Q	K	C	T	L	S	I	S	V	L	L	A	Q	T	I	F	L	F	L	I	A	Q	K
δ	E	S	M	S	T	A	I	S	V	L	L	A	Q	A	V	F	L	L	L	T	S	Q	R
			XENOPUS																				
δ	E	K	M	T	L	A	I	S	V	L	L	A	Q	S	V	F	L	L	L	I	S	Q	R

FIGURE 1. Aligned amino acid sequences of the mouse (LaPolla, Mixter-Mayne, and Davidson, 1985; Isenberg, Mudd, Shah, and Merlie, 1986; Yu, Lapolla, and Davidson, 1986; Gardner, 1990), *Torpedo* (Noda, Takahashi, Tanabe, Toyosato, Furutani, Hirose, Asai, Inayama, Miyata, and Numa, 1982; Claudio, Ballivet, Patrick, and Heinemann, 1983; Noda, Takahashi, Tanabe, Toyosato, Kikyotani, Hirose, Asai, Takashima, Inayama, Miyata, and Numa, 1983), and *Xenopus* M2 regions (Baldwin, Yoshihara, Blackmer, Kintner, and Burden, 1988). Amino acids are given by the single letter code. The amino terminus of M2 was labeled position 1′ (Charnet et al., 1990) and corresponds to αMet243, βMet254, γCys252, and δThr257 in terms of the total sequence numbers. Subunits are indicated at left and the position number in M2 is indicated above the sequence.

Previous data show that 75 μM niflumic acid and 100 μM atropine sulphate do not affect P_{Tris}/P_{Na} (Cohen et al., 1992). Finally, 3 mM Ba^{2+} was added to suppress an increase in the background conductance in the K^+, Cs^+, and Rb^+ solutions. Control experiments indicated that 3 mM Ba^{2+} did not affect P_K/P_{Na} or P_{Cs}/P_{Na}.

The organic chemicals were purchased from Sigma Chemical Co. (St. Louis, MO), Aldrich Chemical Co. (Milwaukee, WI), Fisher Scientific Co. (Pittsburgh, PA), Boehringer Mannheim

Corp. (Indianapolis, IN), and the United States Biochemical Corp. (Cleveland, OH). They were typically ≥98% pure.

We used the Tukey HSD test to detect significant differences between multisample means (Zar, 1984). Statistical tests were performed with the SYSTAT V.4 software (Systat Inc., Evanston, IL).

TABLE I

Permeability Ratios of αβγδ and Frog Endplate Receptors

X^+	R_x	αβγδ	Frog
		P_x/P_{Na} ± SD (n)	P_x/P_{Na}
	Å		
Li^+	0.9	0.98 ± 0.02 (5)	0.87
K^+	1.5	1.16 ± 0.06 (17)	1.11
Rb^+	1.7	1.31 ± 0.13 (8)	1.30
Cs^+	1.8	1.22 ± 0.06 (14)	1.42
Ammonium	1.7	1.97 ± 0.16 (8)	1.79
Hydroxylammonium (pH 5.1)	1.8	2.01 ± 0.19 (5)	1.92
Methylammonium	1.8	1.28 ± 0.04 (7)	1.34
Ethylammonium	2.3	1.45 ± 0.14 (10)	0.72
Dimethylammonium	2.3	1.11 ± 0.08 (16)	0.87
Ethanolammonium	2.4	0.87 ± 0.04 (10)	0.72
Guanidinium	2.4	6.4 ± 1.9 (26)	1.59
n-Propylammonium	2.4	1.35 ± 0.11 (5)	0.68
Piperazinium (pH 7.0)	2.5	0.32 ± 0.02 (5)	0.30
n-Butylammonium	2.6	3.10 ± 0.50 (5)	0.43
Trimethylammonium	2.6	0.50 ± 0.02 (7)	0.36
Diethylammonium	2.6	1.05 ± 0.12 (5)	0.38
Methylethanolammonium	2.6	0.63 ± 0.04 (9)	0.44
Methylguanidinium	2.7	4.24 ± 0.63 (9)	0.79
GME^+ (pH 6.0)	2.7	0.65 ± 0.06 (10)	0.23
n-Amylammonium	2.8	0.00 (4)	ND*
Diethanolammonium	2.8	0.34 ± 0.02 (5)	0.25
Tetramethylammonium	2.9	0.20 ± 0.07 (10)	ND
GEE^+ (pH 5.8)	2.9	0.57 ± 0.06 (10)	0.12
N,N-Dimethylethanolammonium	3.0	0.36 ± 0.02 (9)	0.38‡
Choline	3.2	0.22 ± 0.03 (3)	0.13‡
$Tris^+$	3.3	0.36 ± 0.04 (59)	0.18
Diethylethanolammonium	3.5	0.27 ± 0.11 (7)	0.15
Triethanolammonium	3.6	0.15 ± 0.03 (11)	0.03‡
L-Arginine	3.7	0.04 ± 0.01 (10)	<0.014‡

R_x's for the alkali metal cations are crystal radii taken from Shannon (1976). R_x's for the organic cations were measured from Cory-Pauling-Korn models. P_x/P_{Na} for αβγδ was measured at 23–25°C. P_x/P_{Na} of frog endplate receptors for organic cations was measured at 12°C and taken from Table 2 of Dwyer et al. (1980) unless otherwise noted; P_x/P_{Na} for alkali metals taken from Adams et al. (1980). P_{TMA}/P_{Na} and $P_{amylammonium}/P_{Na}$ for frog endplate receptors were unavailable. The pH of the solution containing the test cation (X^+) is given in parentheses in column 1 for αβγδ if it differs from 7.4. See Dwyer et al. (1980) for the pH of the test solutions for frog receptors. P_{Tris}/P_{Na} for αβγδ was taken from Cohen et al. (1992).

*No data.

‡From Table 3 of Dwyer et al. (1980).

Dimensions of the Organic Cations

As in previous studies of nAChR permeability (Huang et al., 1978; Dwyer et al., 1980), we abstracted the effective radius (R_X) of the organic cations from the dimensions (D_1, D_2, and D_3) of the smallest rectangular box that could contain the space-filling model of the cation:

$$R_X = \frac{\sqrt[3]{D_1 D_2 D_3}}{2}$$

We assumed that all the amines except the quaternary amines (choline and TMA^+) could form a single hydrogen bond with the amino acid residues in the channel; hydrogen bonding reduced the length of a single dimension by ≤ 0.4 Å. We measured the dimensions of only one particular conformation of the molecule and no effort was made to find the most compact conformation. Table I gives R_X for the 25 organic cations we tested. For the most part, our measurements were comparable to previous unpublished estimates used by Dwyer et al. (1980) that were generously supplied to us by Dr. David Adams (University of Miami, Miami, FL).

RESULTS

We measured the permeability ratios of 3 wild-type ($\alpha\beta\gamma\delta$, $\alpha\beta\delta\epsilon$, $(\alpha\beta\gamma\delta)_T$), 1 mouse *Xenopus* hybrid ($\alpha\beta\gamma\delta_X$), 2 subunit-deficient ($\gamma_0$, δ_0), and 22 mutated receptors for a variety of organic and alkali metal cations. The results are summarized in Tables I–III. Table I gives the data for the mouse wild-type, $\alpha\beta\gamma\delta$; Tables II and III give the data for the other receptors tested except the results for Rb^+, which did not warrant inclusion in a table but are described in the text. Previous measurements of permeability ratios for frog endplate receptors (taken from Dwyer et al., 1980) are also listed in Table I for comparison with $\alpha\beta\gamma\delta$. The data for frog endplate receptors were obtained at a lower temperature (12°C) than the data for $\alpha\beta\gamma\delta$ (23–25°C).

The mutations were made at five positions in M2 thought to face the pore, positions −1′, 2′, 6′, 10′, and 14′ (Giraudat et al., 1986; Oberthür et al., 1986; Imoto et al., 1988; Leonard et al., 1988; Charnet et al., 1990; Oiki, Madison, and Montal, 1990; Revah et al., 1990; Konno et al., 1991; Villarroel et al., 1991) and at one position thought to face away from the pore (position 12′). The results show that mutations at positions 2′, 6′, and 10′ and replacement of δ with δ_X ($\alpha\beta\gamma\delta_X$) affected the permeability ratios for several organic cations. Only mutations at position 2′, omission of the δ subunit (δ_0), and substitution of δ_X for δ affected the alkali metal permeability ratios. Consistent with previous experiments using $Tris^+$ (Cohen et al., 1992), we also found a difference between the relative permeability of $\alpha\beta\gamma\delta$ and $(\alpha\beta\gamma\delta)_T$ to diethylammonium.

Guanidinium, glycine methyl ester (GME^+), and glycine ethyl ester (GEE^+) were unusual among the organic cations tested because some mutations actually increased their relative permeabilities. Fig. 2 shows the structures of these cations.

Position 2′ Mutations Affect the Permeability Ratios for Several Organic Cations in Addition to $Tris^+$

Our previous results (Cohen et al., 1992) show that a variety of mutations at position 2′ affect the relative permeability of $\alpha\beta\gamma\delta$ to $Tris^+$. Consistent with these results, we found that three position 2′ mutations ($\alpha\beta\gamma\delta_{S2'T}$, $\alpha\beta\gamma\delta_{S2'F}$, $\alpha_{T2'A}\beta_{G2'S}\gamma_{T2'A}\delta$) which

TABLE II

Organic Permeability Ratios for the Mutated and Subunit-substituted Receptors

Receptor	P_{Tris}/P_{Na}	X^+	P_X/P_{Na} ± SD (*n*)
$\alpha\beta\gamma\delta_{S2'T}$	0.11*	Guanidinium	12.2 ± 4.5 (16)* ↑
		Ethylammonium	1.42 ± 0.21 (11)
		Ethanolammonium	0.68 ± 0.12 (10)* ↓
$\alpha\beta\gamma\delta_{S2'F}$	0.15*	Hydroxylammonium (pH 5.1)	2.24 ± 0.05 (3)
		Diethanolammonium	0.24 ± 0.03 (4)* ↓
		Piperazinium (pH 7.0)	0.14 ± 0.03 (2)* ↓
$\alpha\beta\gamma_{T2'F}\delta$	0.25*	Guanidinium	9.8 ± 2.0 (11)
		Tetramethylammonium	0.16 ± 0.04 (8)
$\alpha_{T2'A}\beta_{G2'S}\gamma_{T2'A}\delta$	0.26*	Hydroxylammonium (pH 5.1)	2.36 ± 0.23 (4)
		GEE^+ (pH 5.8)	0.76 ± 0.07 (9)
		GME^+ (pH 6.0)	0.65 ± 0.03 (9)
		N,N-Dimethylethanolammonium	0.29 ± 0.03 (9)* ↓
$\alpha_{T2'A}\beta\gamma\delta$	0.27*	L-Arginine	0.03 ± 0.01 (9)
$\alpha_{T2'A}\beta\gamma_{T2'A}\delta$	0.27*	Hydroxylammonium (pH 5.1)	1.85 ± 0.20 (4)
$\alpha_{S6'A}\beta\gamma\delta_{S6'A}$	0.30	*n*-Butylammonium	2.22 ± 0.68 (11)
		GEE^+ (pH 5.8)	0.81 ± 0.15 (8)‡ ↑
		Tetramethylammonium	0.16 ± 0.03 (9)
$\alpha\beta\gamma_{T2'S}\delta$	0.31	Guanidinium	6.02 ± 0.54 (4)
		n-Butylammonium	3.16 ± 0.32 (4)
		Ammonium	2.07 ± 0.10 (4)
		Tetramethylammonium	0.16 ± 0.04 (4)
		Triethanolammonium	0.15 ± 0.01 (11)
$\alpha\beta_{F14'Y}\gamma\delta$	0.34	*n*-Propylammonium	1.20 ± 0.18 (6)
		GME^+ (pH 6.0)	0.61 ± 0.06 (6)
$\alpha\beta\gamma\delta_{S6'F}$	0.34	Hydroxylammonium (pH 5.1)	2.04 ± 0.22 (3)
		Diethanolammonium	0.29 ± 0.07 (3)
		Piperazinium (pH 7.0)	0.31 ± 0.03 (2)
$\alpha_{S10'A}\beta_{T10'A}\gamma\delta$	0.35	Diethylammonium	1.30 ± 0.42 (5)
	0.35	GEE^+ (pH 5.8)	1.08 ± 0.39 (6)* ↑
		GME^+ (pH 6.0)	0.93 ± 0.20 (6)* ↑
$\alpha\beta_{F6'S}\gamma\delta$	0.37	Guanidinium	10.9 ± 2.6 (16)
		n-Butylammonium	2.59 ± 0.59 (16)
		Ethanolammonium	0.84 ± 0.05 (3)
$\alpha\beta\gamma\delta_X$	0.05*	Guanidinium	14.3 ± 5.2 (5)* ↑
$(\alpha\beta\gamma\delta)_T$	0.23*	Diethylammonium	2.45 ± 0.29 (3)* ↑
$\alpha\beta\delta\epsilon_5$	0.32	L-Arginine	0.03 ± 0.01 (3)
$\alpha\beta\delta\epsilon$	0.33	L-Arginine	0.03 ± 0.01 (7)
γ_0	0.33	L-Arginine	0.04 ± 0.01 (4)

Measurements of P_{Tris}/P_{Na} taken from Cohen et al. (1992). The arrows beside the permeability ratios in column 4 indicate whether the permeability ratios were significantly larger (↑) or smaller (↓) than the values for $\alpha\beta\gamma\delta$.

*$P < 0.01$ compared with $\alpha\beta\gamma\delta$.

‡$P < 0.05$ compared with $\alpha\beta\gamma\delta$.

reduce P_{Tris}/P_{Na} by 28–69% (Cohen et al., 1992) also significantly ($P < 0.05$) altered the permeability ratios for several other organic cations (Table II).

The $\alpha\beta\gamma\delta_{S2'T}$ mutation reduced $P_{ethanolammonium}/P_{Na}$ by 22%; however, it increased $P_{guanidinium}/P_{Na}$ twofold (Tables I and II). Fig. 3 is an example of *I-V* relations for $\alpha\beta\gamma\delta_{S2'T}$ and for $\alpha\beta\gamma\delta$ in ethanolammonium and Na^+. Complete replacement of Na^+

with ethanolammonium shifted V_r for $\alpha\beta\gamma\delta_{S2'T}$ more negatively than it shifted V_r for $\alpha\beta\gamma\delta$. On average, complete replacement of Na^+ with ethanolammonium shifted V_r for $\alpha\beta\gamma\delta$ by -4 ± 1 mV (mean ± SD, $n = 10$) but shifted V_r for $\alpha\beta\gamma\delta_{S2'T}$ by -10 ± 4 mV ($n = 10$). When 98 mM guanidinium and 2 mM Na^+ were substituted for 100 mM Na^+, V_r shifted by $+46 \pm 8$ mV for $\alpha\beta\gamma\delta$ ($n = 26$) but V_r shifted by $+62 \pm 9$ mV for $\alpha\beta\gamma\delta_{S2'T}$ ($n = 16$).

The $\alpha\beta\gamma\delta_{S2'F}$ mutation reduced the relative permeability of piperazinium nearly twofold and the relative permeability of diethanolammonium by 29% as shown by Tables I and II and the following data. When 98 mM piperazinium was substituted for 100 mM Na^+, V_r shifted by -29 ± 2 mV for $\alpha\beta\gamma\delta$ ($n = 5$) but by -51 ± 6 mV for $\alpha\beta\gamma\delta_{S2'F}$ ($n = 2$). Complete replacement of Na^+ with diethanolammonium shifted V_r for $\alpha\beta\gamma\delta$ by -28 ± 1 mV ($n = 5$), but shifted V_r for $\alpha\beta\gamma\delta_{S2'F}$ by -37 ± 3 mV ($n = 4$). The comparable mutation at position 6' ($\alpha\beta\gamma\delta_{S6'F}$) did not affect $P_{diethanolammonium}/P_{Na}$ or $P_{piperazinium}/P_{Na}$ (Table II).

TABLE III

Permeability Ratios For Li^+, K^+, and Cs^+

Receptor	P_{Cs}/P_{Na} ± SD (n)	P_K/P_{Na} ± SD (n)	P_{Li}/P_{Na} ± SD (n)
$\alpha\beta\gamma\delta$	1.22 ± 0.06 (14)	1.16 ± 0.06 (17)	0.98 ± 0.02 (5)
$\alpha_{T2'A}\beta\gamma\delta_{S2'A}$	1.00 ± 0.10 (7)*	1.11 ± 0.12 (7)	0.98 ± 0.07 (7)
$\alpha\beta\gamma_{T2'\gamma}\delta$	1.08 ± 0.08 (10)	1.00 ± 0.09 (10)	0.98 ± 0.07 (10)
$\alpha\beta\gamma_{T2'F}\delta$	1.09 ± 0.04 (4)‡	0.98 ± 0.10 (6)§	0.96 ± 0.04 (4)
$\alpha\beta\gamma\delta_{F14'E}$	1.12 ± 0.17 (3)	1.04 ± 0.11 (3)	0.92 ± 0.11 (3)
$\alpha_{T2'A}\beta_{G2'S}\gamma\delta$	1.13 ± 0.04 (3)	1.13 ± 0.04 (3)	1.03 ± 0.02 (3)
$\alpha\beta\gamma\delta_{S2'A}$	1.13 ± 0.05 (11)	1.13 ± 0.08 (10)	0.92 ± 0.04 (10)
$\alpha\beta\gamma\delta_{S2'T}$	1.15 ± 0.11 (31)	1.05 ± 0.10 (14)	0.87 ± 0.10 (16)
$\alpha_{T2'A}\beta\gamma_{T2'A}\delta$	1.16 ± 0.06 (6)	1.12 ± 0.08 (7)	ND
$\alpha\beta\gamma_{T2'S}\delta$	1.18 ± 0.04 (8)	1.05 ± 0.06 (12)	0.91 ± 0.04 (9)
$\alpha\beta_{F6'S}\gamma\delta$	1.21 ± 0.06 (9)	1.01 ± 0.16 (8)	0.96 ± 0.04 (8)
$\alpha_{S10'A}\beta_{T10'A}\gamma\delta$	1.22 ± 0.07 (7)	1.11 ± 0.08 (7)	0.96 ± 0.04 (7)
$\alpha_{S10'A}\beta\gamma_{T12'A}\delta$	1.24 ± 0.05 (7)	1.19 ± 0.11 (7)	1.00 ± 0.04 (7)
$\alpha\beta\gamma_{F14'\gamma}\delta$	1.24 ± 0.06 (13)	1.15 ± 0.04 (13)	0.98 ± 0.04 (12)
$\alpha\beta_{F14'\gamma}\gamma\delta$	1.25 ± 0.06 (7)	1.15 ± 0.05 (7)	1.00 ± 0.04 (7)
$\alpha_{S6'A}\beta\gamma\delta_{S6'A}$	1.26 ± 0.08 (14)	ND	0.91 ± 0.10 (7)
$\alpha\beta\gamma_{F14'S}\delta$	1.27 ± 0.07 (6)	1.16 ± 0.07 (7)	0.95 ± 0.06 (8)
$\alpha\beta\gamma\delta_{S6'F}$	1.28 ± 0.09 (5)	1.17 ± 0.09 (13)	0.92 ± 0.16 (6)
$\alpha_{T2'A}\beta_{G2'S}\gamma_{T2'A}\delta$	1.29 ± 0.03 (5)	1.19 ± 0.03 (5)	1.01 ± 0.02 (14)
$\alpha\beta_{G2'S}\gamma\delta$	1.29 ± 0.11 (8)	1.23 ± 0.11 (9)	1.02 ± 0.08 (8)
$\alpha\beta\gamma_{Q-1'E}\delta$	1.33 ± 0.04 (9)	1.24 ± 0.08 (9)	1.00 ± 0.04 (9)
$\alpha\beta\gamma\delta_{S2'F}$	ND	ND	0.94 ± 0.04 (6)
$\alpha\beta\gamma\delta_X$	0.77 ± 0.10 (14)*	0.96 ± 0.12 (12)	0.81 ± 0.09 (8)§
δ_0	1.03 ± 0.21 (14)*	1.11 ± 0.16 (14)	1.02 ± 0.19 (12)
$(\alpha\beta\gamma\delta)_T$	1.18 ± 0.05 (6)	1.09 ± 0.04 (5)	0.91 ± 0.02 (6)
γ_0	ND	1.24 ± 0.18 (4)	ND
$\alpha\beta\delta\epsilon$	ND	1.25 ± 0.16 (4)	0.99 ± 0.09 (4)

*$P < 0.01$ compared with $\alpha\beta\gamma\delta$.
‡$P < 0.1$ compared with $\alpha\beta\gamma\delta$.
§$P < 0.05$ compared with $\alpha\beta\gamma\delta$.

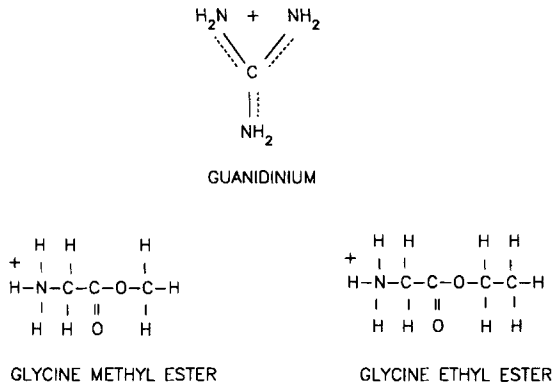

FIGURE 2. Structural formulas of guanidinium and protonated glycine methyl (GME^+) and ethyl ester (GEE^+).

The $\alpha_{T2'A}\beta_{G2'S}\gamma_{T2'A}\delta$ mutation reduced the relative permeability of *N,N*-dimethylethanolammonium ($DMETA^+$) by 19% (Tables I and II). Complete replacement of Na^+ with $DMETA^+$ shifted V_r for $\alpha\beta\gamma\delta$ by -26 ± 2 mV ($n = 9$) but shifted V_r for $\alpha_{T2'A}\beta_{G2'S}\gamma_{T2'A}\delta$ by -32 ± 3 mV ($n = 9$). Three position 2′ mutations ($\alpha_{T2'A}\beta\gamma\delta$, $\alpha\beta\gamma_{T2'F}\delta$, $\alpha_{T2'A}\beta\gamma_{T2'A}\delta$) that produce small (25–31%) reductions in P_{Tris}/P_{Na} and a single position 2′ mutation that does not affect P_{Tris}/P_{Na} (Cohen et al., 1992) also did not measurably affect other organic permeability ratios. These results show that position 2′ mutations affect the permeability ratios for several organic cations; however, $Tris^+$ is a more sensitive indicator of changes at position 2′ than are some of the smaller organic cations.

Position 6′ and 10′ Mutations Affect P_{GME}/P_{Na} and P_{GEE}/P_{Na}

Surprisingly, two double mutations at positions 6′ ($\alpha_{S6'A}\beta\gamma\delta_{S6'A}$) and 10′ ($\alpha_{S10'A}\beta_{T10'A}\gamma\delta$) that affect block by QX-222 (Leonard et al., 1988; Charnet et al.,

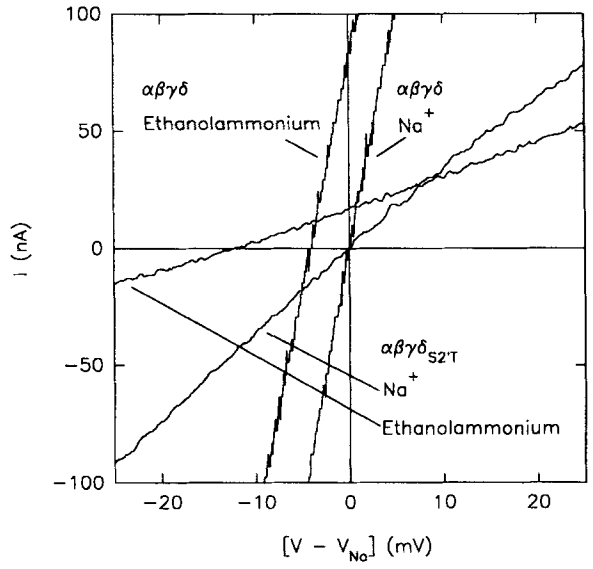

FIGURE 3. Relative permeability of $\alpha\beta\gamma\delta_{S2'T}$ to ethanolammonium. To facilitate comparison, macroscopic current–voltage (*I-V*) relations for the wild-type receptor ($\alpha\beta\gamma\delta$) and $\alpha\beta\gamma\delta_{S2'T}$ in ethanolammonium and Na^+ were translated horizontally so that $V_r = 0$ mV in Na^+. Horizontal line is $I = 0$ nA. In ethanolammonium, $V_r = -4$ mV for $\alpha\beta\gamma\delta$ and $V_r = -12$ mV for $\alpha\beta\gamma\delta_{S2'T}$. [ACh] = 5 μM in Na^+ and [ACh] = 10 μM in ethanolammonium for $\alpha\beta\gamma\delta$. [ACh] = 2 mM for $\alpha\beta\gamma\delta_{S2'T}$.

1990) but not P_{Tris}/P_{Na} (Cohen et al., 1992) increased the relative permeabilities of one or both of the large organic cations, GME^+ and GEE^+ (Tables I and II). The structures of GME^+ and GEE^+ are shown in Fig. 2. The $\alpha_{S6'A}\beta\gamma\delta_{S6'A}$ double mutation increased the relative permeability to GEE^+ by 42%. Substituting 98 mM GEE^+ and 4 mM Na^+ for 100 mM Na^+ shifted V_r for $\alpha\beta\gamma\delta$ by -13 ± 3 mV ($n = 10$) but shifted V_r for $\alpha_{S6'A}\beta\gamma\delta_{S6'A}$ by only -5 ± 4 mV ($n = 8$). The $\alpha_{S10'A}\beta_{T10'A}\gamma\delta$ double mutation increased the relative permeability of GME^+ by 43% and the relative permeability of GEE^+ nearly twofold. For instance, in the experiment of Fig. 4, substituting 98 mM GEE^+ and 4 mM Na^+ for 100 mM Na^+ produced a negative shift in V_r for $\alpha\beta\gamma\delta$ but a small positive shift in V_r for $\alpha_{S10'A}\beta_{T10'A}\gamma\delta$. On average, ΔV_r for GEE^+ was $+1 \pm 8$ mV for $\alpha_{S10'A}\beta_{T10'A}\gamma\delta$ ($n = 6$) but was -13 ± 3 mV for $\alpha\beta\gamma\delta$ ($n = 10$). Substituting 98 mM GME^+ and 5 mM Na^+ for 100 mM Na^+ shifted V_r for $\alpha\beta\gamma\delta$ by -10 ± 2 mV ($n = 10$) but shifted V_r for $\alpha_{S10'A}\beta_{T10'A}\gamma\delta$ by -2 ± 5 mV ($n = 6$). These results show

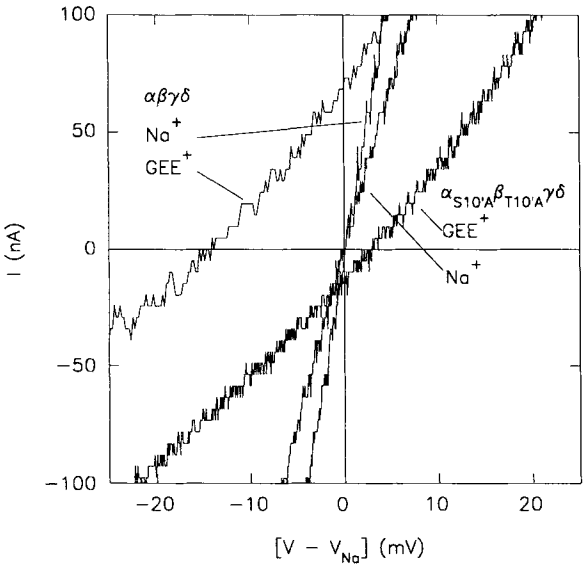

FIGURE 4. Relative permeability of $\alpha_{S10'A}\beta_{T10'A}\gamma\delta$ to glycine ethyl ester (GEE^+). *I-V* relations for $\alpha\beta\gamma\delta$ and $\alpha_{S10'A}\beta_{T10'A}\gamma\delta$ in 100 mM Na^+ (pH 5.7) and in 98 mM GEE^+/4 mM Na^+ (pH 5.8) were translated horizontally so that $V_r = 0$ mV in Na^+. In GEE^+, $V_r = -14$ mV for $\alpha\beta\gamma\delta$ and $V_r = +5$ mV for $\alpha_{S10'A}\beta_{T10'A}\gamma\delta$. [ACh] = 0.5 μM in Na^+ and [ACh] = 20 μM in GEE^+ for $\alpha\beta\gamma\delta$. [ACh] = 0.5 μM in Na^+ and [ACh] = 10 μM in GEE^+ for $\alpha_{S10'A}\beta_{T10'A}\gamma\delta$.

that mutations at other positions in M2 besides $-1'$ and $2'$ can affect organic permeability ratios.

Position 2' Mutations Affect Alkali Metal Permeability Ratios

Previous data show that mutations at position $2'$ affect the relative single-channel conductance of rat muscle nAChRs for alkali metals (Villarroel et al., 1991) and the single-channel conductance of *Torpedo* nAChRs in symmetrical KCl (Imoto et al., 1991). However, there are no data on the effects of position $2'$ mutations on alkali metal permeability ratios.

Of the 21 mutations listed in Table III, only two position $2'$ mutations ($\alpha\beta\gamma_{T2'F}\delta$, $\alpha_{T2'A}\beta\gamma\delta_{S2'A}$) that reduce P_{Tris}/P_{Na} by 31 and 69% (Cohen et al., 1992) significantly affected the relative permeabilities of the alkali metal cations. The $\alpha_{T2'A}\beta\gamma\delta_{S2'A}$ mutation reduced P_{Cs}/P_{Na} by 22% but left P_K/P_{Na} and P_{Li}/P_{Na} unaffected. Fig. 5

shows examples of *I-V* relations for $\alpha\beta\gamma\delta$ (Fig. 5 *A*) and $\alpha_{T2'A}\beta\gamma\delta_{S2'A}$ (Fig. 5 *B*) in Na^+ and Cs^+. V_r for $\alpha\beta\gamma\delta$ shifted to a more positive value after complete replacement of Na^+ with Cs^+. However, $\alpha_{T2'A}\beta\gamma\delta_{S2'A}$ displayed a slightly more negative V_r in Cs^+ than in Na^+ in the experiment of Fig. 5 *B*. The mean shift in V_r for $\alpha_{T2'A}\beta\gamma\delta_{S2'A}$ after complete replacement of Na^+ with Cs^+ was actually 0 ± 2 mV (n = 6) but the mean

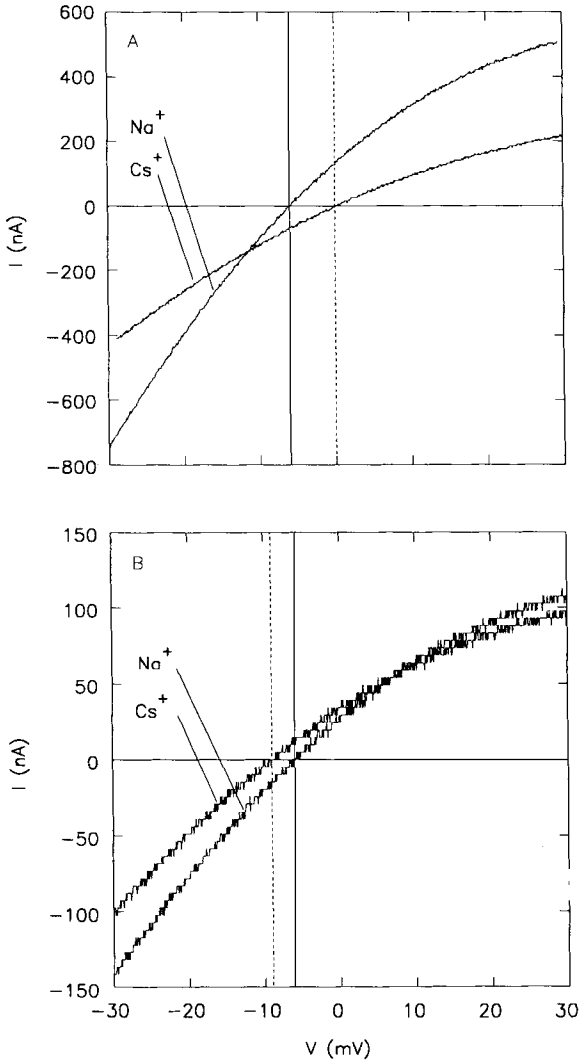

FIGURE 5. Relative permeability of $\alpha_{T2'A}\beta\gamma\delta_{S2'A}$ to Cs^+. Solid vertical lines indicate V_r in Na^+ and dashed vertical lines indicate V_r in Cs^+. Horizontal line is I = 0 nA. (*A*) *I-V* relations for $\alpha\beta\gamma\delta$ in 100 mM Na^+ and 100 mM Cs^+. V_r = −6 mV in Na^+ and V_r = 0 mV in Cs^+. [ACh] = 1 μM. (*B*) *I-V* relations for $\alpha_{T2'A}\beta\gamma\delta_{S2'A}$ in Na^+ and Cs^+. V_r = −6 mV in Na^+ and V_r = −9 mV in Cs^+. [ACh] = 30 μM.

shift in V_r for $\alpha\beta\gamma\delta$ was +5 ± 1 mV (n = 14). A comparable mutation to $\alpha_{T2'A}\beta\gamma\delta_{S2'A}$ at position 6′ ($\alpha_{S6'A}\beta\gamma\delta_{S6'A}$) did not affect P_{Cs}/P_{Na} significantly (Table III). The $\alpha\beta\gamma_{T2'F}\delta$ mutant reduced P_K/P_{Na} by 16% and P_{Cs}/P_{Na} by a marginally significant 11% ($P < 0.1$), but it did not affect P_{Li}/P_{Na}. These results suggest that position 2′ presents a significant permeation barrier to alkali metal cations.

P_{Li}/P_{Na}, P_K/P_{Na}, and P_{Cs}/P_{Na} for the mutations listed in Table III without significant effects on these permeability ratios were in the ranges 0.87–1.03, 1.00–1.24, and 1.08–1.33, respectively. Only three mutations ($\alpha\beta\gamma_{T2'S}\delta$, $\alpha\beta\gamma\delta_{S2'T}$, and $\alpha\beta\gamma_{F14'S}\delta$) were tested with Rb^+ and none affected P_{Rb}/P_{Na}, which ranged from 1.16 to 1.27 (n = 6–11). The addition of a negative charge to position 14′ ($\alpha\beta\gamma\delta_{F14'E}$) or to position −1′ ($\alpha\beta\gamma_{Q-1'E}\delta$) had no effect on P_{Li}/P_{Na}, P_K/P_{Na}, or P_{Cs}/P_{Na} (Table III). Previous data show that adding a negative charge at position −1′ in the *Torpedo* receptor $(\alpha\beta\gamma_{Q-1'E}\delta)_T$ does not affect relative single-channel conductance in symmetrical solutions of alkali metal cations (Konno et al., 1991).

Subunit Alterations That Reduce P_{Tris}/P_{Na} Affect the Permeability Ratios for Other Organic and Metal Cations

We found previously that subunit deletions or substitutions can dramatically reduce the relative permeability of the wild-type mouse nAChR to $Tris^+$ (Cohen et al., 1992). In this study we found that omission of δ from the mRNA injection mixture (δ_0) or substitution of δ_X for δ ($\alpha\beta\gamma\delta_X$), which reduce P_{Tris}/P_{Na} approximately sixfold (Cohen et al., 1992), also affected the permeability ratios of other organic (Table II) and alkali metal cations (Table III).

Substituting δ_X for δ had dramatic effects on ion selectivity. Of 24 receptors, $\alpha\beta\gamma\delta_X$ displayed the least relative permeability to Cs^+ and it was the only receptor that displayed a P_{Li}/P_{Na} that was significantly different ($P < 0.05$) from $\alpha\beta\gamma\delta$. Fig. 6 shows the effect of $\alpha\beta\gamma\delta_X$ on the shift in V_r produced by complete replacement of Na^+ with Cs^+. For comparison, the data for $\alpha\beta\gamma\delta$ in Na^+ and Cs^+ from Fig. 4 *A* are replotted in Fig. 6 *A*. Fig. 6 *B* shows an example of *I-V* relations for $\alpha\beta\gamma\delta_X$ in Na^+ and Cs^+. In contrast to $\alpha\beta\gamma\delta$, $\alpha\beta\gamma\delta_X$ displayed a more negative V_r in Cs^+ than in Na^+. The negative shift in V_r, after substituting Cs^+ for Na^+, was more pronounced for $\alpha\beta\gamma\delta_X$ than for $\alpha_{T2'A}\beta\gamma\delta_{S2'A}$ (see Fig. 4). On average, complete replacement of Na^+ with Cs^+ shifted V_r for $\alpha\beta\gamma\delta$ by +5 ± 1 mV (n = 14) but shifted V_r for $\alpha\beta\gamma\delta_X$ by −7 ± 4 mV (n = 14). Complete replacement of Na^+ with Li^+ shifted V_r for $\alpha\beta\gamma\delta$ by −1 ± 2 mV (n = 5) but shifted V_r for $\alpha\beta\gamma\delta_X$ by −6 ± 3 mV (n = 8). Thus, substitution of δ_X for δ reduced P_{Cs}/P_{Na} by 37% and P_{Li}/P_{Na} by 17%. There were no effects on P_K/P_{Na} (Table III) or P_{Rb}/P_{Na} (n = 3). Substitution of δ_X for δ increased $P_{guanidinium}/P_{Na}$ more than twofold (Table II). Mean ΔV_r after substituting 98 mM guanidinium and 2 mM Na^+ for 100 mM Na^+ was +66 ± 10 mV for $\alpha\beta\gamma\delta_X$ (n = 5) but was +46 ± 8 mV for $\alpha\beta\gamma\delta$ (n = 26). The effect of $\alpha\beta\gamma\delta_X$ on $P_{guanidinium}/P_{Na}$ was similar to the effect of $\alpha\beta\gamma\delta_{S2'T}$ on $P_{guanidinium}/P_{Na}$ (Table II). This mutation mimics $\alpha\beta\gamma\delta_X$ at position 2′ (see Fig. 1).

Omission of δ (δ_0) reduced P_{Cs}/P_{Na} by 16% ($P < 0.01$) but did not significantly affect P_K/P_{Na} or P_{Li}/P_{Na} (Table III). The stoichiometry of the δ_0 receptor appears to be α:β:γ = 2:1:2 (Sine and Claudio, 1991); therefore, δ_0 should mimic the $\alpha\beta\gamma\delta_{E-1'Q}$ mutation at position −1′ (see Fig. 1). Previous data show that the $(\alpha\beta\gamma\delta_{E-1Q})_T$ mutation reduces P_{Cs}/P_{Na} $[(P_{Cs}/P_K)/(P_{Na}/P_K)]$ for *Torpedo* receptors by 26% (Konno et al., 1991). Thus, the effects of δ_0 on P_{Cs}/P_{Na} are consistent with the effects of point mutations at position −1′. Subunit alterations that fail to affect P_{Tris}/P_{Na}—omitting γ from the mRNA injection mixture (γ_0) or substituting ε ($\alpha\beta\delta\varepsilon$), or a 5× concentration of ε ($\alpha\beta\delta\varepsilon_5$) for γ (Cohen et al., 1992)—also failed to affect the permeability ratios of other ions (Tables II and III). None of the mutations or subunit alterations affected P_{Arg}/P_{Na} (Table II) or increased the alkali metal permeability ratios significantly (Table III).

αβγδ Displays an Unusual Permeability Sequence for the Primary Ammonium Series

The permeability sequence of αβγδ for the primary ammonium series of cations shows that αβγδ is not acting as a simple molecular sieve. Fig. 7*A* shows how increasing the length (l) of the hydrocarbon chain attached to NH_4^+ affected the permeability ratios of αβγδ and of frog endplate receptors for a series of primary

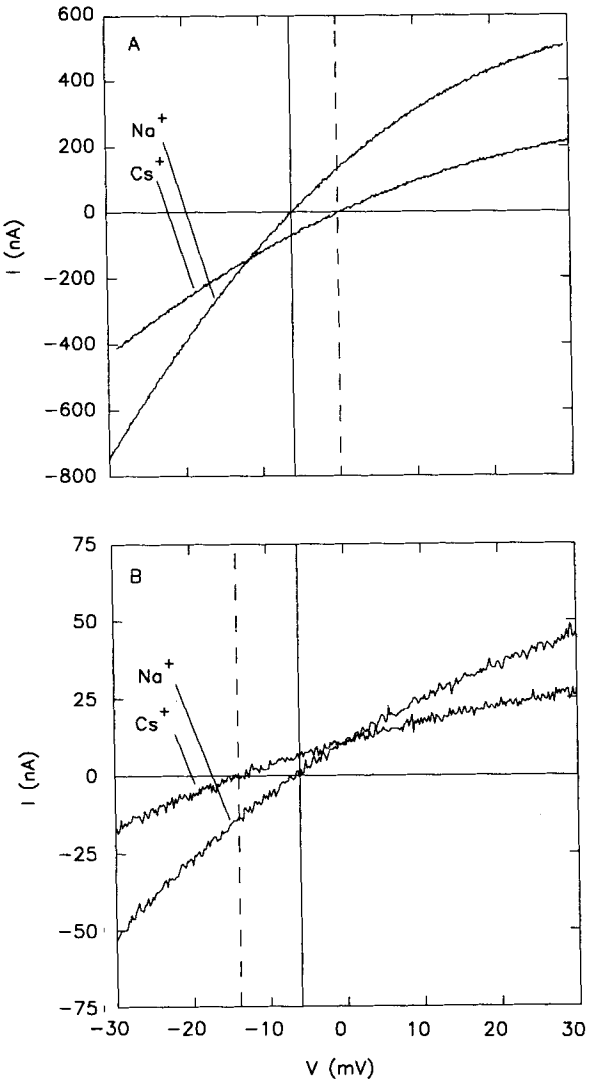

FIGURE 6. Relative permeability of $\alpha\beta\gamma\delta_X$ to Cs^+. Horizontal and vertical lines are the same as in Fig. 4. (*A*) Same as Fig. 4*A*. (*B*) *I-V* relations for $\alpha\beta\gamma\delta_X$ in Na^+ and Cs^+. To facilitate comparison between αβγδ and $\alpha\beta\gamma\delta_X$, the *I-V* relation for $\alpha\beta\gamma\delta_X$ was translated −7 mV horizontally to match V_r for αβγδ in Na^+. After translation, $V_r = -14$ mV in Cs^+. [ACh] = 1 mM.

ammonium ions [NH_4^+ and $(CH_3)(CH_2)_lNH_3$]. In contrast to the previously measured frog permeability ratios (taken from Dwyer et al., 1980), the αβγδ permeability ratios did not decline monotonically with l. The αβγδ permeability ratios declined ~35% between NH_4^+ ($l = 0$) and methylammonium ($l = 1$), increased more than twofold

between n-propylammonium and n-butylammonium (l = 4), and declined precipitously between n-butylammonium and amylammonium (l = 5). We considered amylammonium impermeant because substituting 98 mM amylammonium for 100 mM Na^+ abolished the response of αβγδ to 0.1–1 mM ACh. n-Butylammonium and NH_4^+ have roughly equivalent minimal silhouettes but $P_{butylammonium}/P_{Na}$ exceeded $P_{ammonium}/P_{Na}$, which suggests that the high relative permeability for n-butylammonium is not simply due to a favorable alignment of n-butylammonium with the pore axis.

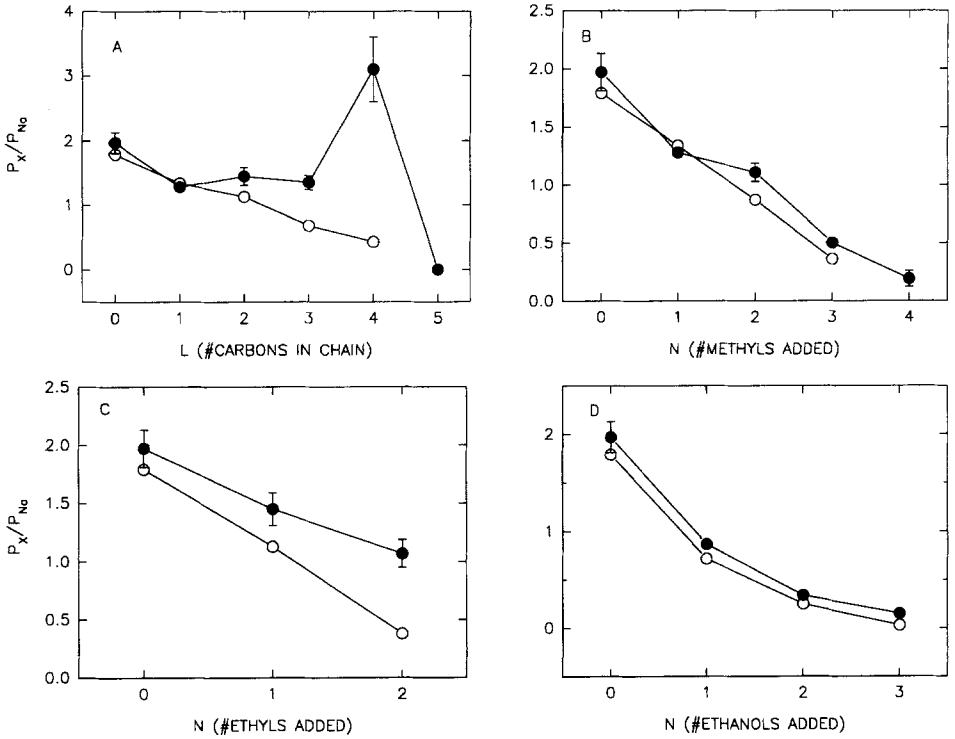

FIGURE 7. Permeability ratios depend on the number (n) of organic substituents or the length (l) of the hydrocarbon chain attached to NH_4^+. Filled circles are αβγδ and open circles are frog permeability ratios (taken from Dwyer et al., 1980). Bars denote one SD. SDs for frog endplate receptors were unavailable. Bars are included for all αβγδ points but are obscured by the data points themselves in some cases. N = 0 and l = 0 represent NH_4^+. (A) P_X/P_{Na} for the primary ammonium series [NH_4^+ and $(CH_3)(CH_2)_lNH_3^+$]. (B) P_X/P_{Na} for the methylammonium series [$(CH_3)_nNH_{(4-n)}^+$]. (C) P_X/P_{Na} for ethylammonium series [$(CH_3H_2)_nNH_{(4-n)}^+$]. (D) P_X/P_{Na} for the ethanolammonium series [$(CH_2OHCH_2)_n\ NH_{(4-n)}^+$].

Unlike the permeability sequence for the primary ammonium series, the relative permeabilities of the methylammonium ($(CH_3)_nNH_{(4-n)}^+$; Fig. 7 B), ethylammonium ($(CH_3CH_2)_n\ NH_{(4-n)}^+$; Fig. 7 C), ethanolammonium ($(CH_2OHCH_2)_n\ NH_{(4-n)}^+$; Fig. 7 D), alkylethanolammonium ($CH_2OHCH_2NH_{(3-n)}\ (CH_3)_n^+$; Fig. 8 A), and dialkyl-

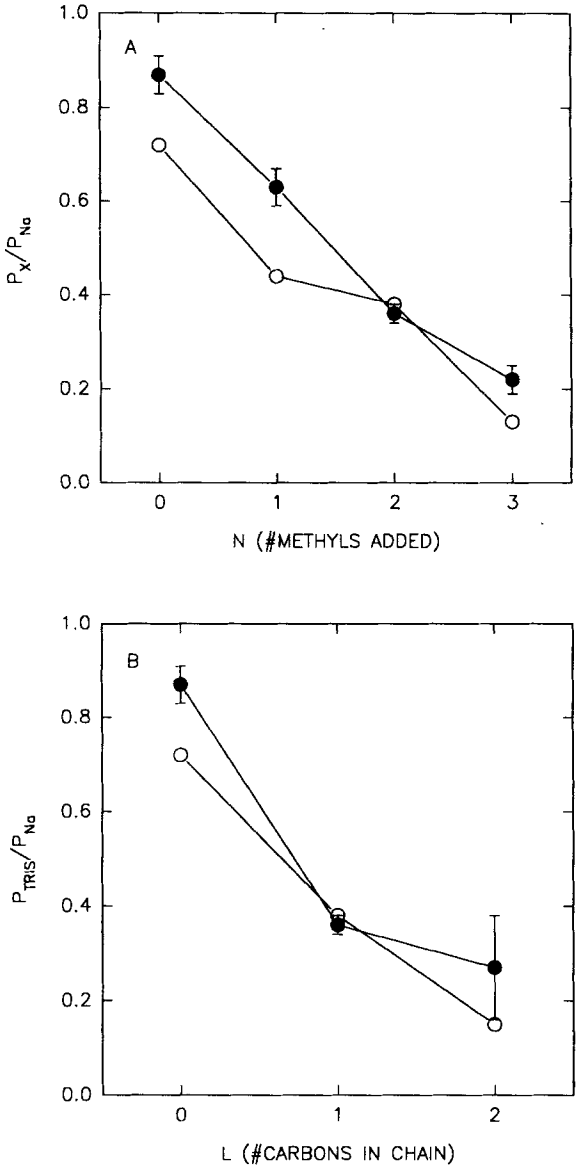

FIGURE 8. Permeability ratios depend on the number (n) of organic substituents or the length (l) of the hydrocarbon chain attached to ethanolammonium. Data for αβγδ (*filled circles*) and for frog endplate receptors (*open circles*). $N = 0$ and $l = 0$ represent ethanolammonium ($CH_2OHCH_2NH_3^+$). (*A*) P_X/P_{Na} for the alkylethanolammonium series [$(CH_2OHCH_2NH_{(3-n)}(CH_3)_n^+$]. (*B*) P_X/P_{Na} for the dialkylethanolammonium series [$CH_2OHCH_2NH(C_lH_{(2l+1)})_2^+$].

ethanolammonium ($CH_2OHCH_2NH(C_lH_{(2l+1)})_2^+$; Fig. 8 *B*) series of cations declined monotonically as the size of the cations increased. The only significant discrepancy between αβγδ and the frog endplate receptor for these cations was that the permeability ratio declined less between NH_4^+ and diethylammonium for αβγδ than for frog endplate receptors (Fig. 8 *C*). Increasing the length (l) or number (n) of the organic substituents attached to NH_4^+ increases molecular volume regardless of the particular conformation that the molecule adopts when permeating the channel. Therefore, these permeability sequences (Figs. 7, *B–D* and 8, *A* and *B*), with the

possible exception of the ethylammonium series (Fig. 8 *C*), are consistent with a simple excluded-area model of ion selectivity.

The αβγδ Pore Narrows to a Diameter of 8.4 Å

We used the permeability ratios for the organic cations (methylammonium, ethanolammonium, alkylethanolammonium, and dialkylethanolammonium series) that were consistent qualitatively with excluded-area theory to estimate the diameter of the narrowest part of the αβγδ pore. In excluded-area theory, the permeability of an ion is proportional to the area of the narrowest region of pore left unoccupied by the ion as it passes through the pore (Dwyer et al., 1980). P_X/P_{Na} is given by:

$$\frac{P_X}{P_{Na}} = \left(\frac{R_c - R_X}{R_c - R_{Na}}\right)^2$$

where R_c, R_X, and R_{Na} are the effective radii of the channel, cation X^+, and Na^+. A convenient transformation of this equation is to take the square root of P_X/P_{Na},

$$\sqrt{\frac{P_X}{P_{Na}}} = a - bR_X$$

where

$$a = \frac{R_c}{R_c - R_{Na}} \tag{1a}$$

$$b = \frac{1}{R_c - R_{Na}} \tag{1b}$$

Excluded-area theory correctly predicts the dependence of $(P_X/P_{Na})^{1/2}$ on R_X for the 12 ammonium cations shown in Fig. 9 *A* and for most of the 25 organic cations (including $Tris^+$) shown in Fig. 9 *B*. The exceptions are guanidinium, methylguanidinium, *n*-butylammonium, and amylammonium. The permeability ratios for guanidinium, methylammonium, and *n*-butylammonium were larger than expected and the permeability ratio for amylammonium was smaller than expected. We can obtain a and b in Eqs. 1a and 1b from the slope and y intercept of the regression line in Fig. 9, *A* and *B*; $a = 2.1 \pm 0.2$ Å^{-1} (± standard error of estimate, SEE) and $b = 0.50 \pm 0.06$ for αβγδ. Using previous data for the 12 cations shown in Fig. 9 *A* for the frog endplate receptor (Dwyer et al., 1980), we obtained a value of 2.2 ± 0.1 Å^{-1} for a and 0.56 ± 0.04 for b (using the estimates of R_X in Table I). These values lead to a pore diameter ($2a/b$) of 8.4 Å for the narrowest portion of αβγδ and 7.9 Å for the narrowest portion of the frog endplate receptor. The pore diameter estimated previously for the frog endplate receptor by Dwyer et al. (1980) was 7.4 Å, very near our estimate using the measurements of R_X given in Table I. $R_{Na} = (a - 1)/b$ was 2.1 Å for both αβγδ and frog endplate receptors, close to the value of 2.15 Å for the hydrated radius of Na^+ in bulk water (Kielland, 1937) and consistent with the observation that limiting equivalent conductance of Na^+ in water is approximately equal to that of dimethylammonium (Robinson and Stokes, 1965), which has an R_X of 2.3 Å (Table I).

$P_{diethylammonium}/P_{Na}$ was more than twofold larger for $(\alpha\beta\gamma\delta)_T$ (Table II) than for $\alpha\beta\gamma\delta$ (Table I), while P_{Tris}/P_{Na} was nearly twofold less for $(\alpha\beta\gamma\delta)_T$ than for $\alpha\beta\gamma\delta$ (Cohen et al., 1992). From the permeability ratios for diethylammonium and $Tris^+$ alone, excluded-area analysis gave a diameter of 7.2 Å for the narrowest part of the

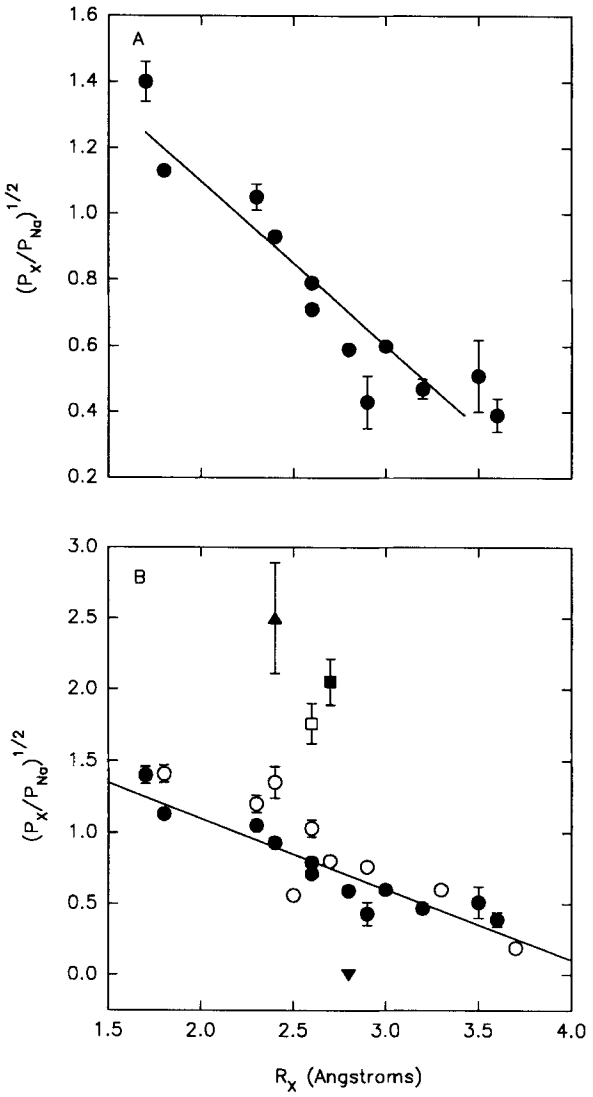

FIGURE 9. $(P_X/P_{Na})^{1/2}$ versus the effective radius (R_X) of the organic cations. R_X and P_X/P_{Na} are taken from Table I. Bars show one SD but are obscured by the points in some cases. Lines represent an unweighted, linear, least-squares fit of $(P_X/P_{Na})^{1/2}$ to R_X for the 12 cations shown in *A* (r = 0.93). (*A*) $(P_X/P_{Na})^{1/2}$ versus R_X for the methylammonium (Fig. 7 *B*), ethanolammonium (Fig. 7 *D*), alkylethanolammonium (Fig. 8 *A*), and dialkylethanolammonium (Fig. 8 *B*) series of cations. (*B*) $(P_X/P_{Na})^{1/2}$ versus R_X for all 25 organic cations tested with $\alpha\beta\gamma\delta$. Points in *A* are replotted as filled circles. Cations with anomalous permeability ratios are as follows: guanidinium (*filled triangle*), methylguanidinium (*filled square*), *n*-butylammonium (*open square*), and amylammonium (*filled inverted triangle*). Open circles are the remaining nine cations in Table I.

$(\alpha\beta\gamma\delta)_T$ channel and a diameter of 8.5 Å for the narrowest part of the $\alpha\beta\gamma\delta$ channel. The effective radius of Na^+ was 3.0 Å for $(\alpha\beta\gamma\delta)_T$ and 2.7 Å for $\alpha\beta\gamma\delta$. The $\alpha\beta\gamma\delta$ pore diameter obtained from P_{Tris}/P_{Na} and $P_{diethylammonium}/P_{Na}$ was consistent with the 8.4-Å diameter obtained from excluded-area analysis of the 12 organic permeability

ratios in Fig. 9*A*. Thus, excluded-area analysis using permeant organic cations gives pore diameters of 7.2–8.4 Å for the wild-type nAChRs.

Temperature Affects $P_{butylammonium}/P_{Na}$ and $P_{guanidinium}/P_{Na}$

Table I shows that there are a number of significant differences between the organic permeability ratios measured at 23–25°C for αβγδ and the corresponding permeability ratios measured previously at 12°C for frog endplate receptors. Previous data suggest that the permeability ratios of nAChRs for alkali metals are independent of temperature from 2–27°C (Hoffmann and Dionne, 1983). However, there are no data on the temperature dependence of the organic permeability ratios of nicotinic receptors. To determine whether temperature could account for some of the differences between the organic permeability ratios of αβγδ and frog endplate receptors, we measured the relative permeability of αβγδ at 13°C to the two organic cations, guanidinium and *n*-butylammonium, that displayed the greatest divergence in permeability ratios between αβγδ and frog endplate receptors. Lowering the temperature from 23–25°C to 13°C reduced $P_{guanidinium}/P_{Na}$ by 38% and $P_{butylammonium}/P_{Na}$ by 62%. Replacement of 100 mM Na^+ with 98 mM guanidinium and 2 mM Na^+ shifted V_r by +46 ± 8 mV (n = 26) at 23–25°C but by +34 ± 2 mV (n = 10) at 13°C. Thus, $P_{guanidinium}/P_{Na}$ was 6.4 ± 1.9 (n = 26) at 23–25°C (Table I) and 4.00 ± 0.42 (n = 10) at 13°C. Complete replacement of Na^+ by *n*-butylammonium shifted V_r by +29 ± 4 mV (n = 5) at 23–25°C and by +4 ± 1 mV (n = 7) at 13°C. $P_{butylammonium}/P_{Na}$ was 3.11 ± 0.50 (n = 5) at 23–25°C (Table I) and 1.17 ± 0.07 (n = 7) at 13°C. In contrast, $P_{guanidinium}/P_{Na}$ is 1.59 and $P_{butylammonium}/P_{Na}$ is 0.43 for frog endplate receptors at 12°C (Dwyer et al., 1980). Therefore, $P_{guanidinium}/P_{Na}$ and $P_{butylammonium}/P_{Na}$ for αβγδ at 13°C are higher than the corresponding permeability ratios for frog endplate receptors at 12°C.

$P_{guanidinium}/P_{Na}$ was somewhat variable at 23–25°C. Two factors contribute to the variability of $P_{guanidinium}/P_{Na}$ for αβγδ at 23–25°C (Table I). The first factor is that the transformation of ΔV_r into a permeability ratio (P_X/P_{Na}) increases the coefficient of variation if $\Delta V_r > 0$. The second factor is that the background conductance became more variable at depolarized potentials. However, only a background current that is systematically activated or inhibited by ACh in guanidinium and has a different relative permeability to guanidinium than the mouse nAChR would bias the mean value of ΔV_r for guanidinium. The experiments with *d*-TC discussed below show that there is no such current.

An Alternative Measurement Procedure Also Yields Large $P_{guanidinium}/P_{Na}$ and $P_{butylammonium}/P_{Na}$

We performed an additional series of experiments to show that nicotinic receptors give rise to the surprisingly high values of $P_{guanidinium}/P_{Na}$ and $P_{butylammonium}/P_{Na}$ listed in Tables I and II. We compared V_r for I_{ACh} with V_r for the fraction of I_{ACh} sensitive to *d*-TC. The *d*-TC-sensitive current was measured by subtracting the current activated by ACh in the presence of *d*-TC from the total ACh-activated current. V_r for I_{ACh} in guanidinium or in *n*-butylammonium was not significantly different from V_r for the *d*-TC-sensitive fraction of I_{ACh}. In guanidinium, I_{ACh} reversed at +62 ± 3 mV and the *d*-TC-sensitive I_{ACh} reversed at +62 ± 9 mV (n = 6). At a concentration of 100 μM,

d-TC blocked >80% of the response to 100 μM ACh. In *n*-butylammonium, I_{ACh} reversed at +17 ± 2 mV and the *d*-TC-blocked I_{ACh} reversed at +12 ± 5 mV (n = 6).

Amylammonium and n-Propylammonium Block αβγδ

To determine how far amylammonium enters into the channel, we analyzed the block of αβγδ by 1 mM amylammonium (Fig. 10, *A–C*). For comparison, we also examined block by the permeant primary ammonium, *n*-propylammonium, which blocks frog endplate channels (Adams, Nonner, Dwyer, and Hille, 1981).

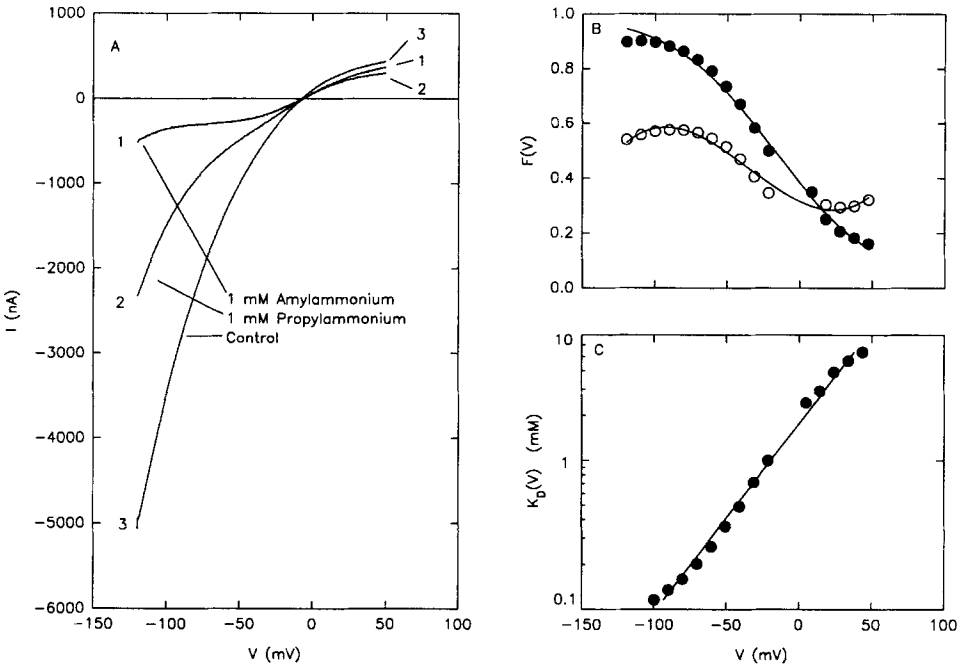

FIGURE 10. Block of αβγδ by 1 mM amylammonium and by 1 mM *n*-propylammonium. (*A*) Effect of amylammonium and *n*-propylammonium on the *I-V* relation for αβγδ in 100 mM Na^+ (*Control*). [ACh] = 2 μM. Horizontal line is I = 0 nA. (*B*) Fraction of the ACh response ($F(V)$) blocked by amylammonium (*filled circles*) and by *n*-propylammonium (*open circles*) versus membrane potential. Curve was fit to amylammonium data using the Woodhull theory (see text). Curve for the *n*-propylammonium data is a third-order polynomial least-squares regression and simply indicates the trend in the data points. (*C*) Semilog plot of the apparent dissociation constant ($K_D(V)$) for amylammonium versus voltage. Straight line represents the regression of $\log[K_D(V)]$ against voltage. $K_D(0)$ = 1.6 mM. F_b = 0.7.

Both 1 mM amylammonium and 1 mM *n*-propylammonium blocked I_{ACh} in a voltage-dependent manner (Fig. 10*A*). Fig. 10*B* shows the fraction [$F(V)$] of the control current [$I_c(V)$] blocked by 1 mM amylammonium and by 1 mM *n*-propylammonium as a function of voltage,

$$F(V) = 1 - \frac{I_b(V)}{I_c(V)}$$

where $I_b(V)$ is I_{ACh} at voltage V in the presence of the blocker. Block by amylammonium was more voltage dependent than block by *n*-propylammonium. These data suggest that amylammonium can enter the αβγδ pore. The weaker voltage sensitivity and the relief of the *n*-propylammonium block at high negative potentials presumably occur because this cation is permeant and can leave its binding site toward either the inside or the outside face of the pore. Block by *n*-propylammonium was not analyzed further. The relief of the amylammonium block at very negative membrane potentials (less than −100 mV) suggests that amylammonium may be slightly permeant even though it cannot carry a detectable current through the channel.

We used the Woodhull (1973) model to determine the location of the amylammonium binding site in the electric field of the channel. This formulation has proven useful for many open-channel blockers (Lester, 1992); based on such analysis it is reasonable to assume that (*a*) the channel is nonconducting when amylammonium occupies its binding site, (*b*) block by amylammonium is in rapid equilibrium during the voltage ramp used to generate the *I-V* relation, and (*c*) amylammonium binding follows conventional first-order kinetics. Then

$$K_D(V) = \frac{[\text{amylammonium}]}{F(V)} - 1$$

where $K_D(V)$ is the dissociation constant for amylammonium binding to the channel as a function of voltage. Assuming an infinitely high inner permeation barrier for the blocking cation, the Woodhull (1973) model predicts that

$$K_D(V) = K_D(0)\theta^{f_b zFV/RT}$$

where f_b (typically termed δ but renamed here to avoid confusion with the δ subunit) is the fraction of the electric field of the channel measured from the extracellular side that amylammonium must cross to reach its binding site. Fig. 10 *B* presents a nonlinear least-squares fit of the amylammonium data to the Woodhull model. Fig. 10 *C* shows that, as predicted by this model, $K_D(V)$ was an exponential function of voltage between −100 and +50 mV. We measured $K_D(0)$ and f_b by fitting a regression line to $\log[I_b(V)/[(I_c(V) - I_b(V)]]$ as a function of voltage. $K_D(0)$ was 1.9 ± 0.8 mM and f_b was 0.8 ± 0.1 (n = 9). At −73 mV, $K_D(V)$ was 0.2 mM for amylammonium, which is more than an order of magnitude smaller than the apparent K_D of frog endplate receptors for *n*-propylammonium at this voltage (Adams et al., 1981). Previous data show that f_b for QX-222 is 0.78 for frog extrajunctional nAChRs (Neher and Steinbach, 1978) and f_b for QX-222 falls between 0.65 and 0.8 for αβγδ (Leonard et al., 1988; Charnet et al., 1990). That f_b is similar for amylammonium and QX-222 suggests that amylammonium binds to the same site in M2, position 6′ and 10′, where many channel blockers and local anesthetics bind (Lester, 1992). A permeation barrier at position 2′ could prevent some large organic cations from moving further into the channel.

DISCUSSION

Positions −1′ and 2′ Are the Narrowest Part of the αβγδ Pore

This paper agrees with most other recent structure–function studies in supporting the hypothesis that positions −1′ and 2′ in M2 are the narrowest part of the nAChR

pore (reviewed by Lester, 1992). In our view, the nAChR subunits have an α-helical secondary structure at this region, so that positions −1′ and 2′ are on the same side of an α-helix, approximately one turn apart. Changes in the amino acids at these positions affect single-channel conductance (Imoto et al., 1988, 1991; Konno et al., 1991; Villarroel et al., 1991; Cohen et al., 1992) and ion selectivity (Konno et al., 1991; Cohen et al., 1992). The concept of a single turn as the narrowest region is consistent with streaming potential measurements (Dani, 1989). Moreover, mutations at other positions in M2 (6′, 10′, 12′, and 14′) do not affect P_{Tris}/P_{Na} (Cohen et al., 1992) or alkali metal permeability ratios and mutations at position −4′ and 20′ have smaller effects on single-channel conductance than do mutations at position −1′ (Imoto et al., 1988). The present results show, in addition, that changes in the amino acids at position 2′ ($\alpha\beta\gamma\delta_X$, $\alpha\beta\gamma\delta_{S2'T}$, $\alpha\beta\gamma\delta_{S2'F}$, $\alpha_{T2'A}\beta_{G2'S}\gamma_{T2'A}\delta$) affect the permeability ratios of αβγδ to five different organic cations besides $Tris^+$ and the permeability ratios of αβγδ for alkali metal cations ($\alpha\beta\gamma_{T2'F}\delta$, $\alpha_{T2'A}\beta\gamma\delta_{S2'A}$).

This picture of the pore is consistent with the effects of δ_0 on P_{Cs}/P_{Na}. The stoichiometry of δ_0 appears to be α:β:γ = 2:1:2 (Sine and Claudio, 1991), so that compared with αβγδ, δ_0 has (*a*) one less glutamate residue and one more glutamine at position −1′ and (*b*) one more threonine and one less serine at position 2′ (see Fig. 1). The corresponding mutation at position −1′ in *Torpedo* $(\alpha\beta\gamma\delta_{E-1'Q})_T$ but not the corresponding mutation at position 2′ in mouse ($\alpha\beta\gamma\delta_{S2'T}$) reduces P_{Cs}/P_K (Konno et al., 1991). Thus, the reduction in P_{Cs}/P_{Na} in δ_0 could be the result of changes in the residues at position −1′. The large pore diameter of αβγδ may explain why mutations and subunit alterations have relatively small effects on metal cation selectivity.

Biionic reversal potentials are often used to measure the relative barrier heights of permeant ions (Hille, 1991). Our data and previous work on the *Torpedo* nAChR (Konno et al., 1991) show that changes in the residues at positions −1′ and 2′ alter the biionic reversal potentials for metal cations. Previous data (Konno et al., 1991; Villarroel et al., 1991) show that mutations at these two positions affect the single-channel conductance ratios of the rat (Villarroel et al., 1991) and *Torpedo* (Konno et al., 1991) nAChR for alkali metal cations. Thus, these positions may also be associated with an energy well for metal cations. How can changes at positions −1′ and 2′ affect both barrier height and well depth? According to a recent model of the nAChR (Levitt, 1991), the boundaries of the narrowest region of the nAChR form the two major permeation barriers in the channel, and these barriers are separated by an energy well. Thus, if the residues at positions −1′ and 2′ demarcate the narrowest region of the nAChR, then mutations at these positions could affect both well depth and barrier height. If a well for metal cations exists here, the high flow rate of the nAChR ($\sim 10^7$ ions/s) suggests that the well is not very deep.

Other Positions in M2 Affect Ion Selectivity

Serine or threonine to alanine mutations at positions 6′ and 10′ ($\alpha_{S6'A}\beta\gamma\delta_{S6'A}$, $\alpha_{S10'A}\beta_{T10'A}\gamma\delta$) increase P_{GME}/P_{Na} and P_{GEE}/P_{Na} but do not affect P_{Tris}/P_{Na} (Cohen et al., 1992). Evidently GME and GEE probe an aspect of permeation that $Tris^+$ does not. The effects of position 6′ and 10′ mutations on QX-222 blockade (Leonard et al., 1988; Charnet et al., 1990) suggest a possible explanation for the effects of

$\alpha_{S6'A}\beta\gamma\delta_{S6'A}$ and $\alpha_{S10'A}\beta_{T10'A}\gamma\delta$ on P_{GEE}/P_{Na} and P_{GME}/P_{Na}. Mutations that increase the hydrophobicity of position 10′ increase the affinity of αβγδ for QX-222 (Charnet et al., 1990), while mutations that increase the hydrophobicity of position 6′ reduce the affinity of αβγδ for QX-222 (Leonard et al., 1988). We suggested previously that the aromatic ring of QX-222 binds to position 10′ and the quaternary amine binds to position 6′ (Charnet et al., 1990) because these positions could be separated by ~5.4 Å (the pitch of an α-helix) and lie approximately on the same face of the helix if the secondary structure of M2 is α-helical. Both GME^+ and GEE^+ have a hydrophobic moiety (methyl or ethyl) and a hydrophilic moiety (protonated amine) separated by three atoms (see Fig. 2), which is sufficient to span one turn of an α-helix depending on the exact conformation of the permeant molecule. A pore with appropriately placed hydrophobic and hydrophilic residues could increase the probability that the long axes of GME^+ and of GEE^+ are aligned parallel to the pore axis. If positions 6′ and 10′ are adjacent to the narrowest part of the pore, then such an alignment could reduce the energy required for these cations to pass through the narrowest part of the pore. The $\alpha_{S10'A}\beta_{T10'A}\gamma\delta$ double mutation would therefore increase P_{GME}/P_{Na} and P_{GEE}/P_{Na} because it renders position 10′ more hydrophobic. Position 6′ would function as the hydrophilic site for GME^+ and GEE^+ (see Fig. 1). The $\alpha_{S6'A}\beta\gamma\delta_{S6'A}$ double mutation would increase P_{GEE}/P_{Na} by a similar mechanism, but now position 6′ would interact more strongly with the aromatic moiety and position 2′ with the charged moiety (see Fig. 1).

A comparison of the effects of subunit alterations and point mutations also suggests that positions in M2 besides −1′ and 2′ may influence ion selectivity. For example, substituting δ_X for δ mimics the $\alpha\beta\gamma\delta_{S2'T}$ mutation at position 2′. However, $\alpha\beta\gamma\delta_X$, but not $\alpha\beta\gamma\delta_{S2'T}$, reduces P_{Cs}/P_{Na} and P_{Li}/P_{Na} significantly. Another example is that the difference between P_{Tris}/P_{Na} for $(\alpha\beta\gamma\delta)_T$ and αβγδ is not the result of changes in the amino acids at positions −1′ and 2′ (Cohen et al., 1992). Both δ_X and δ_T have a neutral glutamine residue at position 20′ instead of the positively charged lysine present at the corresponding position in δ (Fig. 1). Previous data show that increasing the positive charge at position 20′ $(\alpha_{E20'K}\beta\gamma\delta)_T$ increases the Cs^+/K^+ single-channel conductance ratio of the *Torpedo* nAChR (Konno et al., 1991). These data suggest that the charged residues at position 20′ may also affect relative permeability. However, there is no direct evidence that mutations at position 20′ affect permeability ratios, and an alternative explanation for discrepancies between the subunit substitutions and point mutations is that subunit substitutions result in conformation changes that are not mimicked by point mutations.

Selectivity of Wild-Type Receptors Varies across Species

At first glance, the ion selectivity of αβγδ for monovalent metal and organic cations resembles the selectivity of other muscle-type nAChRs expressed in native tissue (Huang et al., 1978; Watanabe and Narahashi, 1979; Adams, Dwyer, and Hille, 1980; Dwyer et al., 1980) and in oocytes (Konno et al., 1991). The αβγδ receptor is only weakly selective for alkali metal cations ($|P_X/P_{Na} - 1| \leq 0.3$) and it is permeable to a wide variety of organic cations. As reported previously (Konno et al., 1991), we found that $(\alpha\beta\gamma\delta)_T$ is also relatively nonselective for the alkali metal cations. From a subset of the organic permeability ratios that are consistent with excluded-area theory, we

estimate that the diameter of the narrowest part of the αβγδ channel is 8.4 Å, similar to the diameter we estimate for the narrowest part of the frog endplate channel (7.9 Å) using the same subset of organic cations and previous relative permeability measurements (Dwyer et al., 1980). While it is true that most of the αβγδ organic permeability ratios are larger than the corresponding frog permeability ratios (Dwyer et al., 1980), differences in temperature between the present αβγδ experiments and the frog endplate experiments may account for some of these differences.

Nonetheless, differences between the permeability ratios for guanidinium, *n*-butylammonium, methylguanidinium, $Tris^+$, and diethylammonium suggest that there are structural differences among muscle nAChRs from different species. The guanidinium/Na^+ and *n*-butylammonium/Na^+ permeability ratios are 2.5- and 2.8-fold larger for αβγδ at 13°C than for frog endplate receptors at 12°C (Dwyer et al., 1980). The guanidinium/Cs^+ permeability ratio for nAChRs in chick myotubes is 1.6 at 11°C (Dwyer, 1986). Assuming that P_{Cs}/P_{Na} for chick myotube nAChRs at 11°C equals that for frog endplate receptors at 12°C (P_{Cs}/P_{Na} = 1.4; Adams et al., 1980), then the guanidinium/Na^+ permeability ratio for chick myotube nAChRs would be 1.1 at 11°C, ~ fourfold less than $P_{guanidinium}/P_{Na}$ for αβγδ. Another clear example of the variation in nAChR selectivity across species is the difference between $P_{diethylammonium}/P_{Na}$ and P_{Tris}/P_{Na} for αβγδ and for $(\alpha\beta\gamma\delta)_T$. $P_{diethylammonium}/P_{Na}$ is more than twofold greater for $(\alpha\beta\gamma\delta)_T$ than for αβγδ at 23–25°C. In contrast, P_{Tris}/P_{Na} for $(\alpha\beta\gamma\delta)_T$ is nearly twofold less than P_{Tris}/P_{Na} for αβγδ at 23–25°C (Cohen et al., 1992).

Excluded-Area Theory Cannot Account for Some Permeability Ratios

Excluded-area theory explains the overall correlation between cation size and relative permeability, but some of our data are not consistent with this theory. *n*-Butylammonium, guanidinium, and methylguanidinium have minimal silhouettes that approach NH_4^+, but their permeability ratios exceed $P_{ammonium}/P_{Na}$. Even after allowing for the possibility that these cations might be aligned in the αβγδ pore so that they present a minimal cross-section when they reach the narrowest part of the pore, it is difficult to reconcile their relative permeabilities with an excluded-area model of selectivity. This statement also holds true for more sophisticated excluded-area models that postulate an additional drag factor on permeating ions or a noncircular cross-section for the pore.

The frog endplate receptor is also not perfectly sieve-like (Dwyer et al., 1980). For example, the permeability ratios of the unsaturated organic cations are larger than expected from the excluded-area effect and the permeability ratios for large organic cations are smaller than expected (Dwyer et al., 1980). However, the anomalies are not as pronounced for frog endplate receptors as for αβγδ.

Temperature Affects Relative Permeability

The Q_{10} for the increase in the relative permeability of *n*-butylammonium over the range 13–25°C is 2.6. The Q_{10} for the single-channel conductance of αβγδ over the same range is 1.5 in symmetrical KCl (Cohen et al., 1992) and the Q_{10} for aqueous diffusion is typically 1.3 (Hille, 1991). The similarity between (*a*) the effective radius of Na^+ in the αβγδ pore and in water, and (*b*) the sequence of the relative permeabilities of αβγδ for the alkali metals and their mobilities in water suggests that

movement of Na^+ through the $\alpha\beta\gamma\delta$ resembles diffusion through water. If the Q_{10} of the major permeation barrier for Na^+ resembles the Q_{10} of aqueous diffusion or the Q_{10} of the single-channel conductance of $\alpha\beta\gamma\delta$ in symmetrical K^+, then the Q_{10} of the absolute permeability for *n*-butylammonium is 3.4–3.9.

Our data show that $P_{\text{butylammonium}}/P_{\text{Na}} > 1$ and $P_{\text{butylammonium}}/P_{\text{Na}}$ increases with temperature. One interpretation of these data involves the entropy associated with ion permeation. The rate-limiting step of a reaction depends exponentially on the enthalpy of activation ($\Delta H^{\ddagger}$) (see, for instance, Morris, 1974). According to Eyring models of ion permeation, the X^+/Na^+ permeability ratio represents the ratio of rate constants for cation X^+ and Na^+ to cross the major rate-limiting energy barrier in the channel (Hille, 1975). The free energy of a permeation barrier ($\Delta G^{\ddagger}$) is related to $\Delta H^{\ddagger}$ and the entropy of activation ($\Delta S^{\ddagger}$) as follows:

$$\Delta G^{\ddagger} = \Delta H^{\ddagger} - T\Delta S^{\ddagger}$$

Our data deal only with the ratios P_X/P_{Na}; therefore, we must write

$$\Delta(\Delta G^{\ddagger}) = \Delta(\Delta H^{\ddagger}) - T\Delta(\Delta S^{\ddagger})$$

where $\Delta(\Delta G^{\ddagger})$ refers to the difference between the height of the free energy barrier for cation X^+ and for Na^+ [$\Delta G^{\ddagger}(X)$-$\Delta G^{\ddagger}(Na)$]. Assuming that $\alpha\beta\gamma\delta$ has a single main permeation barrier for *n*-butylammonium and Na^+, $P_{\text{butylammonium}}/P_{\text{Na}} > 1$ implies that $\Delta(\Delta G^{\ddagger}) < 0$ and the positive temperature dependence of $P_{\text{butylammonium}}/P_{\text{Na}}$ implies that $\Delta(\Delta H^{\ddagger}) > 0$. Therefore, $T\Delta(\Delta S^{\ddagger})$ must be $> \Delta(\Delta H^{\ddagger})$ and $\Delta(\Delta S^{\ddagger})$ must be > 0. According to this analysis, the positive entropy term [$\Delta S^{\ddagger}(X) - \Delta S^{\ddagger}(Na)$] is primarily responsible for the greater relative permeability of *n*-butylammonium than Na^+. The positive enthalpy term [$\Delta H^{\ddagger}(X) - \Delta H^{\ddagger}(Na)$] is responsible for the temperature dependence of $P_{\text{butylammonium}}/P_{\text{Na}}$. Our analysis (see Appendix) suggests that $\Delta(\Delta S^{\ddagger})$ for *n*-butylammonium and Na^+ is ~ 0.05 entropy units. Enzyme–substrate binding in solution can result in an increase in entropy through the loss of *intra*molecular hydrogen bonds (i.e., between the enzyme and water or between the substrate and water [Fersht, 1985]) and could provide a possible explanation for the difference in entropy between Na^+ and *n*-butylammonium permeation through the channel. If *n*-butylammonium hydrogen bonds to the residues at the major permeation barrier in the pore (positions $-1'$ and $2'$), then the loss of *intra*molecular hydrogen bonds could account for the favorable relative entropy term in *n*-butylammonium permeation and the anomalously large permeability ratios for this cation, for guanidinium, and for methylguanidinium.

Conclusions

Our results disclose new features of permeation governed by the M2 domains of $\alpha\beta\gamma\delta$ and other muscle-type nAChRs. In addition to effects at positions $-1'$ and $2'$, we found that positions $6'$ and $10'$ affect the permeability ratios for some organic cations. We interpret our results in the context of (*a*) previous data indicating that positions $-1'$ and $2'$ are the narrowest part of the nAChR pore, and (*b*) models suggesting that the boundaries of the narrowest region present the main permeation barriers in the channel; we suggest that positions $6'$ and $10'$ align some permeant

organic cations axially in the pore analogous to the manner in which they bind local anesthetics.

APPENDIX

According to Eyring models of ion permeation, P_X/P_{Na} represents the ratio of the rate constants for cation X^+ and for Na^+ to cross the major rate-limiting energy barrier in the channel (Hille, 1975). The relative Arrhenius activation energy of P_X/P_{Na} (ΔE_a) is related to the P_X/P_{Na} at temperature T_1 [$P_X/P_{Na}(T_1)$] and T_2 [$P_X/P_{Na}(T_2)$] by the following equation (Morris, 1974):

$$\Delta E_a = \frac{2.3RT_1T_2\left[\log \frac{P_X}{P_{Na}}(T_2) - \log \frac{P_X}{P_{Na}}(T_1)\right]}{T_2 - T_1}$$

where R = 1.987 cal K^{-1} mol^{-1}. From the P_X/P_{Na} of αβγδ for guanidinium and *n*-butylammonium at 13°C (286°K) and 23–25°C (297°K), we get an ΔE_a of 7.2 kcal/mol for guanidinium and an ΔE_a of 14.9 kcal/mol *n*-butylammonium. The term $\Delta(\Delta H^\ddagger)$ represents the difference $[\Delta H^\ddagger(X) - \Delta H^\ddagger(Na)]$ between the enthalpy of the major free energy barrier for cation X^+ and Na^+ to permeate the channel. Assuming $\Delta H^\ddagger/\Delta T = 0$ (negligible heat capacity) and using the approximation $E_a = \Delta H^\ddagger + RT$ (Morris, 1974), we get a $\Delta(\Delta H^\ddagger)$ of +6.6 kcal/mol for guanidinium and a $\Delta(\Delta H^\ddagger)$ of +14.3 kcal/mol for *n*-butylammonium at 23–25°C.

The free energy of a permeation barrier ($\Delta G^\ddagger$) is related to $\Delta H^\ddagger$ as follows:

$$\Delta G^\ddagger = \Delta H^\ddagger - T\Delta S^\ddagger$$

where $\Delta S^\ddagger$ is the difference between the entropy of the ground state and the entropy of the transition state. Assuming a single major permeation barrier for αβγδ, the difference between the height of the free energy barrier for cation X^+ and for Na^+ [$\Delta(\Delta G^\ddagger)$] is related to $P_X/P_{Na}(T)$ by the following equation:

$$\Delta(\Delta G^\ddagger) = -2.303\,RT \log \frac{P_X}{P_{Na}}(T)$$

Using the mean values of P_X/P_{Na} for guanidinium ($P_X/P_{Na} = 6.4 \pm 1.9$) and for *n*-butylammonium ($P_X/P_{Na} = 3.11 \pm 0.50$) at 23–25°C (see Table I), $\Delta(\Delta G^\ddagger)$ was −1.1 kcal/mol for guanidinium and −0.7 kcal/mol for *n*-butylammonium. From the two above equations, the difference between the entropy of the free energy barrier for cation X^+ and for Na^+ $\Delta(\Delta S^\ddagger)$ is:

$$\Delta(\Delta S^\ddagger) = \frac{\Delta(\Delta H^\ddagger) - \Delta(\Delta G^\ddagger)}{T}$$

Thus, $\Delta(\Delta S^\ddagger)$ was 0.03 kcal·$mol^{-1}K^{-1}$ for guanidinium and 0.05 kcal·$mol^{-1}K^{-1}$ for *n*-butylammonium. According to this analysis, the positive entropy term $\Delta(\Delta S^\ddagger)$ gives guanidinium and *n*-butylammonium a greater relative permeability than Na^+. The positive relative enthalpy term $\Delta(\Delta H^\ddagger)$ gives P_X/P_{Na} its temperature dependence.

We thank Michael Quick and Linda Czyzyk for technical assistance.

This research was supported by grants from the National Institute of Health (NS-11756), the Muscular Dystrophy Association, and the University of California Tobacco-Related Disease Research Program.

Original version received 5 March 1992 and accepted version received 10 June 1992.

REFERENCES

Adams, P. R. 1975*a*. Drug interactions at the motor endplate. *Pflügers Archiv.* 360:155–164.

Adams, P. R. 1975*b*. Kinetics of agonist conductance changes during hyperpolarization at frog endplates. *British Journal of Pharmacology.* 53:308–310.

Adams, D. J., T. M. Dwyer, and B. Hille. 1980. The permeability of endplate channels to monovalent and divalent metal cations. *Journal of General Physiology.* 75:493–510.

Adams, D. J., W. Nonner, T. M. Dwyer, and B. Hille. 1981. Block of endplate channels by permeant cations in frog skeletal muscle. *Journal of General Physiology.* 78:593–615.

Baldwin, T. J., C. M. Yoshihara, K. Blackmer, C. R. Kintner, and S. J. Burden. 1988. Regulation of acetylcholine receptor transcript expression during development in *Xenopus laevis*. *Journal of Cell Biology.* 106:469–478.

Charnet, P., C. Labarca, R. J. Leonard, N. J. Vogelaar, L. Czyzyk, A. Gouin, N. Davidson, and H. A. Lester. 1990. An open-channel blocker interacts with adjacent turns of α-helices in the nicotinic acetylcholine receptor. *Neuron.* 4:87–95.

Claudio, T., M. Ballivet, J. Patrick, and S. Heinemann. 1983. Nucleotide and deduced amino acid sequences of *Torpedo* californica acetylcholine receptor γ subunit. *Proceedings of the National Academy of Sciences, USA.* 80:1111–1115.

Cohen, B. N., C. Labarca, L. Czyzyk, N. Davidson, and H. A. Lester. 1992. $Tris^+/Na^+$ permeability ratios of nicotinic acetylcholine receptors are reduced by mutations near the intracellular end of the M2 region. *Journal of General Physiology.* 99:545–572.

Dani, J. A. 1989. Open channel structure and ion binding sites of the nicotinic acetylcholine receptor. *Journal of Neuroscience.* 9:884–892.

Dascal, N. 1987. Use of the *Xenopus* oocyte system to study ion channels. *CRC Critical Reviews in Biochemistry.* 22:317–387.

DiPaola, M., P. N. Kao, and A. Karlin. 1990. Mapping the α-subunit site photolabeled by the noncompetitive inhibitor [^{3}H]quinacrine azide in the active state of the nicotinic acetylcholine receptor. *Journal of Biological Chemistry.* 265:11017–11029.

Dwyer, T. M. 1986. Guanidine block of single channel currents activated by acetylcholine. *Journal of General Physiology.* 88:635–650.

Dwyer, T. M., D. J. Adams, and B. Hille. 1980. The permeability of the endplate channel to organic cations in frog muscle. *Journal of General Physiology.* 75:469–492.

Fersht, A. 1985. Enzyme Structure and Mechanism. 2nd ed. W. H. Freeman and Company, New York. 301–302.

Gardner, P. 1990. Nucleotide sequence of the ε-subunit of the mouse muscle nicotinic receptor. *Nucleic Acids Research.* 18:6714.

Giraudat, J., M. Dennis, T. Heidmann, J.-Y. Chang, and J.-P. Changeux. 1986. Structure of the high-affinity binding site for noncompetitive blockers of the acetylcholine receptor: serine-262 of the γ subunit is labeled by [^{3}H]chlorpromazine. *Proceedings of the National Academy of Sciences, USA.* 83:2719–2723.

Giraudat, J., M. Dennis, T. Heidmann, P. Haumont, F. Lederer, and J. P. Changeux. 1987. Structure of the high-affinity binding site for noncompetitive blockers of the acetylcholine receptor: [^{3}H]chlorpromazine labels homologous residues in the β and δ chains. *Biochemistry.* 26:2410–2418.

Giraudat, J., J.-L. Galzi, F. Revah, J.-P. Changeux, P.-Y. Haumont, and F. Lederer. 1989. The noncompetitive blocker [^{3}H]chlorpromazine labels segment M2 but not segment M1 of the nicotinic acetylcholine receptor α-subunit. *FEBS Letters.* 253:190–198.

Hille, B. 1975. Ionic selectivity of Na and K channels of nerve membranes. *In* Membranes: A Series of Advances. Vol. 3. Lipid Bilayers and Biological Membranes: Dynamic Properties. G. Eisenman, editor. Marcel Dekker, Inc., New York. 255–323.

Hille, B. 1991. Ionic Channels in Excitable Membranes. 2nd ed. Sinauer Associates, Inc., Sunderland, MA. 329, 370–371.

Hoffmann, H. M., and V. E. Dionne. 1983. Temperature dependence of ion permeation at the endplate channel. *Journal of General Physiology.* 81:687–703.

Huang, L. M., W. A. Catterall, and G. Ehrenstein. 1978. Selectivity of cations and nonelectrolytes for acetylcholine-activated channels in cultured muscle cells. *Journal of General Physiology.* 71:397–410.

Hucho, F., W. Oberthür, and F. Lottspeich. 1986. The ion channel of the nicotinic acetylcholine receptor is formed by the homologous helices M II of the receptor subunits. *FEBS Letters.* 205:137–142.

Imoto, K., C. Busch, B. Sakmann, M. Mishina, T. Konno, J. Nakai, H. Bujo, Y. Mori, K. Fukuda, and S. Numa. 1988. Rings of negatively charged amino acids determine the acetylcholine receptor channel conductance. *Nature.* 335:645–648.

Imoto, K., T. Konno, J. Nakai, F. Wang, M. Mishina, and S. Numa. 1991. A ring of uncharged polar amino acids as a component of channel constriction in the nicotinic acetylcholine receptor. *FEBS Letters.* 289:193–200.

Imoto, K., C. Methfessel, B. Sakmann, M. Mishina, Y. Mori, T. Konno, K. Fukuda, M. Kurasaki, H. Bujo, Y. Fujita, and S. Numa. 1986. Location of a δ-subunit region determining ion-transport through the acetylcholine-receptor channel. *Nature.* 324:670–674.

Isenberg, K. E., J. Mudd, V. Shah, and J. P. Merlie. 1986. Nucleotide sequence of the mouse muscle nicotinic acetylcholine receptor α subunit. *Nucleic Acids Research.* 14:5111.

Kielland, J. 1937. Individual activity coefficients of ions in aqueous solutions. *Journal of the American Chemical Society.* 56:1675–1678.

Konno, T., C. Busch, E. von Kitzing, K. Imoto, F. Wang, J. Nakai, M. Mishina, S. Numa, and B. Sakmann. 1991. Rings of anionic amino acids as structural determinants of ion selectivity in the acetylcholine receptor channel. *Proceedings of the Royal Society of London, Series B.* 244:69–74.

LaPolla, R. J., K. S. Mixter-Mayne, and N. Davidson. 1985. Isolation and characterization of cDNA clone for the complete coding region of the δ subunit of the mouse acetylcholine receptor. *Proceedings of the National Academy of Sciences, USA.* 81:7970–7984.

Leonard, R. J., C. Labarca, P. Charnet, N. Davidson, and H. A. Lester. 1988. Evidence that the M2 membrane-spanning region lines the ion channel pore of the nicotinic receptor. *Science.* 242:1578–1581.

Lester, H. A. 1992. The permeation pathway of neurotransmitter-gated ion channels. *Annual Review of Biophysics and Biomolecular Structure.* 21:267–292.

Levitt, D. G. 1991. General continuum theory for multiion channel II. Application to acetylcholine channel. *Biophysical Journal.* 59:278–288.

Morris, J. G. 1974. A Biologist's Physical Chemistry. 2nd ed. Edward Arnold, London. 264–271.

Neher, E., and J. H. Steinbach. 1978. Local anesthetics transiently block currents through single acetylcholine-receptor channels. *Journal of Physiology.* 277:153–176.

Noda, M., H. Takahashi, T. Tanabe, M. Toyosato, Y. Furutani, T. Hirose, M. Asai, S. Inayama, T. Miyata, and S. Numa. 1982. Primary structure of α-subunit precursor of *Torpedo californica* acetylcholine receptor deduced from cDNA sequence. *Nature.* 299:793–797.

Noda, M., H. Takahashi, T. Tanabe, M. Toyosato, S. Kikyotani, T. Hirose, M. Asai, H. Takashima, S. Inayama, T. Miyata, and S. Numa. 1983. Primary structures of β and δ subunit precursors of *Torpedo californica* acetylcholine receptor deduced from cDNA sequences. *Nature.* 301:251–255.

Oberthür, W., P. Muhn, H. Baumann, F. Lottspeich, B. Wittmann-Liebold, and F. Hucho. 1986. The reaction site of a non-competitive antagonist in the γ-subunit of the nicotinic acetylcholine receptor. *EMBO Journal.* 5:1815–1819.

Oiki, S., V. Madison, and M. Montal. 1990. Bundles of amphipathic transmembrane α-helices as a structural motif for ion-conducting channel proteins: studies on sodium channels and acetylcholine receptors. *Proteins: Structure, Function, and Genetics.* 8:226–236.

Revah, F., J. Galzi, J. Giraudat, P. Haumont, F. Lederer, and J. P. Changeux. 1990. The non-competitive blocker [^{3}H]chlorpromazine labels three amino acids of the acetylcholine receptor γ subunit: Implications for the α-helical organization of regions MII and for the structure of the ion channel. *Proceedings of the National Academy of Sciences, USA.* 87:4675–4679.

Robinson, R. A., and R. H. Stokes. 1965. Electrolyte Solutions. Butterworth & Co., Ltd., London. 465.

Shannon, R. D. 1976. Revised effective radii and systematic studies of interatomic distances in halides and chalcogenides. *Acta Crystallographica.* A32:751–767.

Sine, S. M., and T. Claudio. 1991. Gamma-subunits and delta-subunits regulate the affinity and the cooperativity of ligand-binding to the acetylcholine-receptor. *Journal of Biological Chemistry.* 266: 19369–19377.

Villarroel, A., S. Herlitze, M. Koenen, and B. Sakmann. 1991. Location of a threonine residue in the α-subunit M2 transmembrane segment that determines the ion flow through the acetylcholine receptor channel. *Proceedings of the Royal Society of London, Series B.* 243:69–74.

Watanabe, S., and T. Narahashi. 1979. Cation selectivity of acetylcholine-activated ionic channel of frog endplate. *Journal of General Physiology.* 74:615–628.

White, M. M., and M. Aylwin. 1990. Niflumic and flufenamic acids are potent blockers of Ca^{2+}-activated Cl^- channels in *Xenopus* oocytes. *Molecular Pharmacology.* 37:720–724.

Woodhull, A. M. 1973. Ionic blockage of sodium channels in nerve. *Journal of General Physiology.* 61:687–708.

Yu, L., R. J. LaPolla, and N. Davidson. 1986. Mouse muscle nicotinic acetylcholine receptor γ subunit: cDNA sequence and gene expression. *Nucleic Acids Research.* 14:3539–3555.

Zar, J. H. 1984. Biostatistical Analysis. Prentice-Hall, Englewood Cliffs, NJ. 186–190.